ACS NANO
Cite This: ACS Nano 2018, 12, 7613–7628
www.acsnano.org

ARTICLE

Human Mesenchymal Stem Cell Derived Exosomes Alleviate Type 2 Diabetes Mellitus by Reversing Peripheral Insulin Resistance and Relieving β-Cell Destruction

Yaoxiang Sun,[†,‡,§] Hui Shi,[†,§] Siqi Yin,[†,§] Cheng Ji,[†] Xu Zhang,[†] Bin Zhang,[†] Peipei Wu,[†] Yinghong Shi,[†] Fei Mao,[†] Yongmin Yan,[†] Wenrong Xu,*[,†] and Hui Qian*[,†]

[†]Jiangsu Key Laboratory of Medical Science and Laboratory Medicine, Institute of Stem Cell, School of Medicine, Jiangsu University, Zhenjiang, Jiangsu 212013, China

[‡]Department of Clinical Laboratory, The Affiliated Yixing Hospital of Jiangsu University, Yixing, Jiangsu 214200, China

Supporting Information

ABSTRACT: **Exosomes are nanosized extracellular vesicles (EVs) that show great promise in tissue regeneration and injury repair as mesenchymal stem cell (MSC). MSC has been shown to alleviate diabetes mellitus (DM) in both animal models and clinical trials. In this study, we aimed to investigate whether exosomes from human umbilical cord MSC (hucMSC-ex) have a therapeutic effect on type 2 DM (T2DM). We established a rat model of T2DM using a high-fat diet and streptozotocin (STZ). We found that the intravenous injection of hucMSC-ex reduced blood glucose levels as a main paracrine approach of MSC. HucMSC-ex partially reversed insulin resistance in T2DM indirectly to accelerate glucose metabolism. HucMSC-ex restored the phosphorylation (tyrosine site) of the insulin receptor substrate 1 and protein kinase B in T2DM, promoted expression and membrane translocation of glucose transporter 4 in muscle, and increased storage of glycogen in the liver to maintain glucose homeostasis. HucMSC-ex inhibited STZ-induced β-cell apoptosis to restore the insulin-secreting function of T2DM. Taken together, exosomes from hucMSC can alleviate T2DM by reversing peripheral insulin resistance and relieving β-cell destruction, providing an alternative approach for T2DM treatment.**

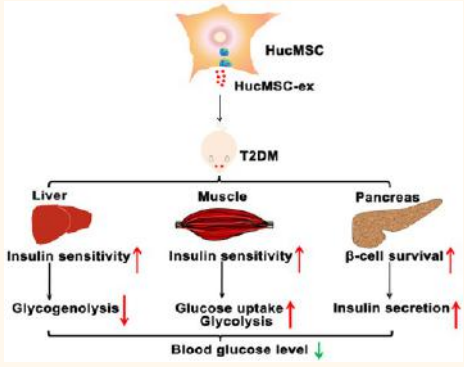

KEYWORDS: *exosomes, mesenchymal stem cell, type 2 diabetes mellitus, insulin sensitivity, glucose metabolism*

Diabetes mellitus (DM) is a metabolic disease that affects an estimated 500 million people worldwide.[1] Type 2 diabetes mellitus (T2DM) accounts for 95% of diabetes cases. Peripheral insulin resistance, pancreatic β-cell mass loss, and β-cell dysfunction are primary causes of T2DM, which results in glucose out of control and degenerative complications.[1,2] Pump or daily insulin injection and chemical drugs, such as sulfonylurea, metformin, and thiazolidinedione, are the current principal treatments for T2DM.[1] However, these treatments can only temporarily control blood glucose levels and have side effects such as ametropia, subcutaneous nodule, diarrhea, and obesity. In addition, exogenous insulin administration may result in the loss of insulin production and secretion in β-cells, making it hard to ameliorate peripheral insulin resistance and relieve the symptoms of diabetic complications.[1,3,4]

The transplantation of tissues and stem cells has been used to improve diabetes care.[5,6] However, the insufficient donation of tissues and low survival rate of stem cells *in vivo* make these approaches unsatisfactory.[7,8] Mesenchymal stem cell (MSC) derived from different tissues such as bone marrow, umbilical cord, and adipose have been currently under investigation for their potential in tissue regeneration.[9−12] The intravenous infusion of bone marrow derived MSC can reverse hyperglycemia in a high-fat diet (HFD) and streptozotocin (STZ)-induced T2DM rat models by improving insulin secretion, activating the insulin-signaling pathway, and increasing the expression and membrane transposition of glucose transporters (GLUT).[13,14] The transfusion of adipose-derived MSC can significantly lower blood glucose levels *via* promoting hepatic glycogen synthesis and inhibiting hepatic glucose production in

Received: October 28, 2017
Accepted: July 25, 2018
Published: July 27, 2018

DOI: 10.1021/acsnano.7b07643
ACS Nano 2018, 12, 7613–7628

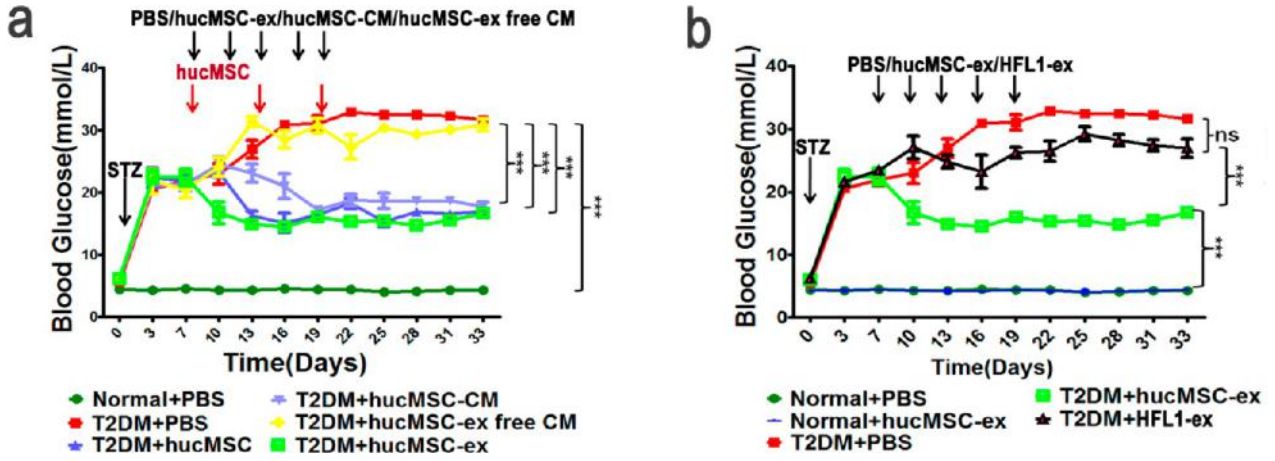

Figure 1. HucMSC-ex down-regulated blood glucose levels in T2DM rats as the main paracrine approach of hucMSC. (a) HucMSC-ex, hucMSC-CM, hucMSC-ex free CM (protein concentration: 10 mg/kg bw), and hucMSC (3×10^6 cells/dose) in 0.2 mL of PBS and 0.2 mL of PBS were infused into five groups of T2DM rats by intravenous tail injection, and the blood glucose levels were determined 3 h after starved, normal rats were treated with PBS as the control (each group compared with T2DM+PBS). (b) HucMSC-ex and HFL1-ex (protein concentration: 10 mg/kg bw) in 0.2 mL of PBS and 0.2 mL of PBS were infused into three groups of T2DM rats by intravenous tail injection, and the blood glucose levels were determined; normal rats were treated with hucMSC-ex (protein concentration: 10 mg/kg bw) in 0.2 or 0.2 mL of PBS as the control (all groups compared with each other). Values in a,b are mean ± SE; $n = 6$ rats per group; ns >0.05, $^{**}p < 0.01$, $^{***}p < 0.001$ determined by repeated measures of ANOVA.

T2DM rats.[15] Moreover, T2DM patients transplanted with human umbilical cord MSC (hucMSC) have shown relatively stable blood glucose levels; some patients become insulin free at 25−43 months after treatment, and others only require a low dose of insulin.[16] Although there is evidence that MSC could be induced into islet endocrine lineages *in vitro*,[17−20] there is also a report showing that MSC cannot differentiate into *β*-cells *in vivo*,[13,21] indicating that MSC may exert their activities in T2DM mostly through paracrine actions.

MSC-derived factors have pleotropic roles in T2DM therapy. The culture medium from BM-MSC can reduce blood glucose levels in T2DM animal models.[14] The conditioned medium (CM) from adipose-derived MSC can reverse insulin resistance *in vitro* by up-regulating GLUT4 levels and reducing interleukin 6 (IL-6) and plasminogen activator inhibitor-1 (PAL-1) levels.[22] Exosomes are extracellular nanoparticles secreted by cells and contain bioactive molecules including proteins, lipids, and nucleic acids.[10,23] Exosomes involved in glucose metabolism in diabetes are attracting attention. Thomou *et al.* have found that adipose-derived exosomes could transfer miR-99b to hepatic cells to regulate the expression of fibroblast growth factor 21 (FGF-21) and participate in glucose metabolism.[24] Garcia *et al.* have found that cardiomyocyte-derived exosomes can directly transfer GLUT protein and glycolytic enzymes to endothelial cells to modulate glucose transport.[25] These studies suggest that exosomes carrying active contents may be the key approach of MSC that mediates their therapeutic effects in diabetes. Although it is known that T2DM is a systematic disease, therapeutic effects of conventional oral medicines are always complicated because of low water solubility or high clearance after "biotransformation"; as one kind of nanomedicine, the efficiency of exosomes should be considered for the physical barriers, as well. Before being internalized by target tissues or cells, exosomes need to escape the clearance of the liver or kidneys to avoid the absorption of serum protein, to escape surveillance of the immune system, and to interact with vascular endothelial walls and the extracellular matrix.[26] After exosomes overcoming these barriers and getting to the target tissue, the exosomes internalized by target cells need to escape the degradation of the endosome/lysosome, which also depends on the size and structure of exosomes.[26,27] The special characteristics of structure ("cup" or "dish" in transmission electron microscopy), size (30−150 nm), and density (1.13−1.19 g/mL)[28] of exosomes allow them to be easily absorbed, to cross the blood−brain barrier or to be internalized by target cells in the caveolae route, which is a much better way for exosomes to escape the degradation of endosome/lysosome,[26] and the lipid bilayer membrane can protect carried components from degradation of the physical environment and provide a long-term releasing effect. This information indicates that exosomes have more advantages than other nanoparticles and may be a potential "smart" nanomedicine for diabetes treatment. We have previously reported that hucMSC-derived exosomes (hucMSC-ex) could repair liver fibrosis,[29,30] acute renal injury,[31] and cutaneous wound healing.[10,11,32] We identified the contents of hucMSC-ex by LC/MS-MS and found that glucose metabolism associated proteins were enriched in hucMSC-ex.[10,32] Therefore, we hypothesized that hucMSC-ex might also alleviate hyperglycemia in T2DM as observed in hucMSC.

In the current study, we exploit the feasibility and efficacy of using hucMSC-ex to alleviate a T2DM rat model induced by HFD and streptozotocin.[33] Results show that intravenous infusion of hucMSC-ex can decrease blood glucose levels in T2DM rats by enhancing insulin sensitivity of the periphery organs and relieving islet destruction. HucMSC-ex can restore glucose homeostasis of T2DM by promoting the expression and membrane translocation of GLUT4 in muscle and glycogen storage in the liver depending on insulin. HucMSC-ex relieved the insulin-secreting dysfunction in T2DM by inhibiting STZ-induced *β*-cell apoptosis. HucMSC-ex shows a desirable alleviating ability in T2DM rat models.

DOI: 10.1021/acsnano.7b07643
ACS Nano 2018, 12, 7613−7628

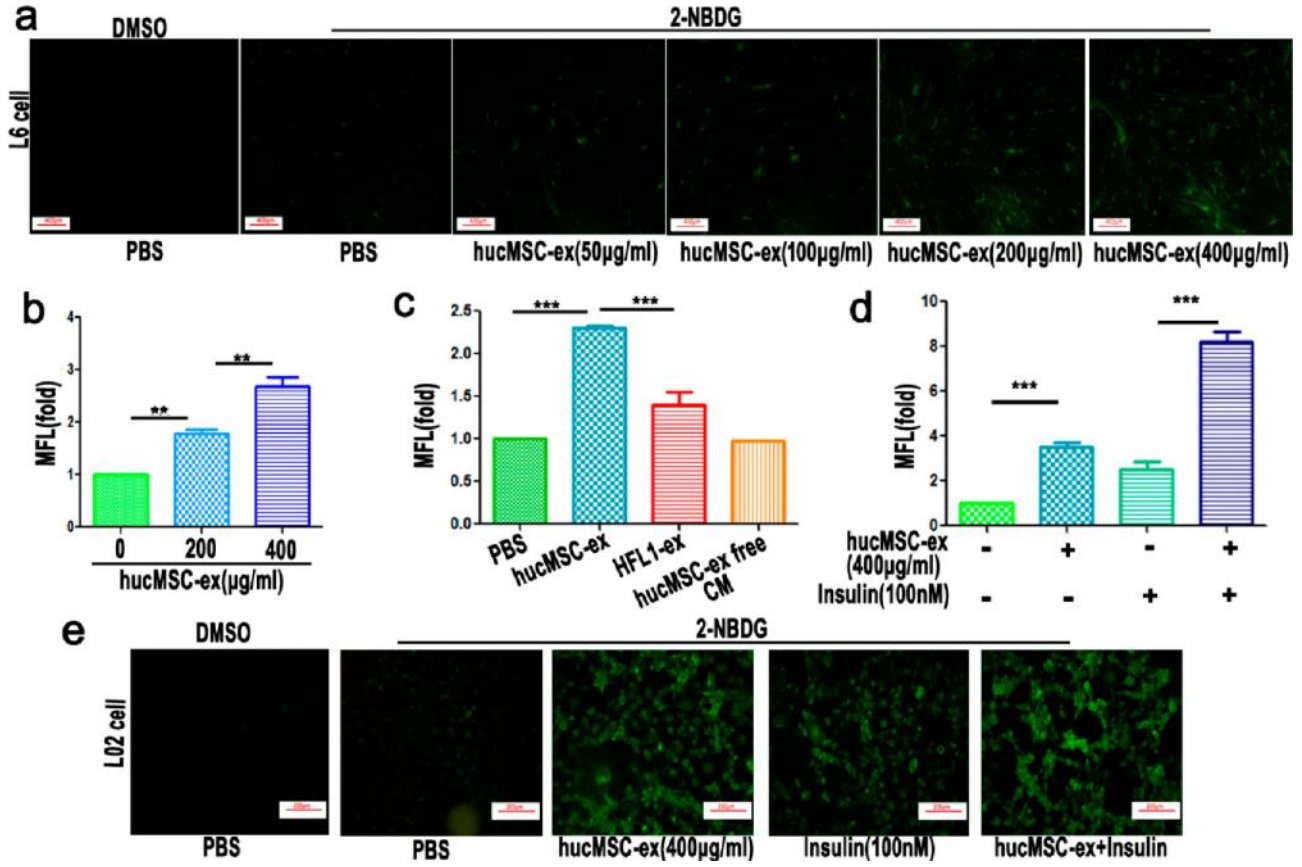

Figure 2. HucMSC-ex enhanced glucose uptake in muscle cells (L6 cells) and hepatic cells (L02 cells). Cell models were pretreated with hucMSC-ex, HFL1-ex, or hucMSC-ex-free CM for 24 h and stimulated with insulin or not for 30 min before incubation with 2-NBDG, DMSO as control. (a) Concentration-dependent effect of hucMSC-ex on 2-NBDG uptake in L6 cells was determined with fluorescence microscopy (scale bar = 400 μm). (b) Effect of hucMSC-ex on 2-NBDG uptake in L6 cells was confirmed by flow cytometry (FCM) (wavelength = 488 nm). (c) Effect of hucMSC-ex, HFL1-ex, and hucMSC-ex-free CM (protein concentration: 400 μg/mL) on 2-NBDG uptake in L6 cells was detected by FCM (wavelength = 488 nm). (d) Effect of insulin (100 nM), hucMSC-ex, and hucMSC-ex + insulin on 2-NBDG uptake in L6 cells was analyzed by FCM (wavelength = 488 nm). (e) Effect of insulin, hucMSC-ex, and hucMSC-ex + insulin on 2-NBDG in L02 cells was observed with fluorescence microscopy (scale bar = 200 μm). Values of b–d are mean ± SE; n = 3 per group; $^{**}p < 0.01$, $^{***}p < 0.001$ determined by one-way ANOVA.

RESULTS AND DISCUSSION

Identification of HucMSC-ex and Fat-Fed/STZ-Induced T2DM Rat Model. HucMSC-ex and human lung fibroblast 1 derived exosomes (HFL1-ex) were purified from cell culture supernatant as previously described[30−32] and characterized by transmission electron microscopy, nanoparticle tracking analysis (NTA), and Western blot. The results showed that hucMSC-ex displayed cup-like morphology (Figure S1a) with a mode diameter of around 120 nm (Figure S1b) and expressed exosomal markers CD9 and CD81 (Figure S1c). HFL1-ex was the control and had similar features. We previously analyzed the protein contents of hucMSC-ex by using LC/MS-MS and identified GLUT, pyruvate kinase (PK), and lactic dehydrogenase (LDH) in hucMSC-ex.[32] We confirmed the enrichment of GLUT4 in hucMSC-ex but not in HFL1-ex (Figure S1c).

To test the therapeutic effects of hucMSC-ex on T2DM, we established a rat model by a HFD combined with STZ.[14,33] T2DM rats showed blood glucose levels higher than 20 mmol/L, but the normal group was lower than 10 mmol/L, regardless if they rats were fasted or re-fed (Figure S2a). Reduced insulin sensitivity, decreased islet size, and impaired serum insulin levels were indicated by the results of oral glucose tolerance tests (OGTTs) (Figure S2b), intraperitoneal insulin tolerant tests (IPITTs) (Figure S2c), pancreas histology (Figure S2d), and serum insulin tests (Figure S2e). In addition, the rats also showed typical symptoms of T2DM, including polyphagia, polydipsia, and polyuria. The data indicated the successful establishment of a T2DM animal model.

HucMSC-ex Ameliorated Hyperglycemia in T2DM Rats. To investigate whether hucMSC-ex has a therapeutic effect on T2DM as hucMSC, we infused hucMSC-ex (10 mg/kg body weight (bw) was the maximum tolerated dose, Figure S3a), hucMSC, and phosphate-buffered saline (PBS) into T2DM rats *via* the tail vein; normal rats were infused with PBS as a control, and the blood glucose levels were detected in different groups every 3 days for 1 month (detailed procedure is in supplementary Table S1). The results of continuous blood glucose tests displayed that hucMSC-ex considerably ameliorated hyperglycemia in T2DM rats as hucMSC (Figure 1a). After the last infusion of hucMSC-ex, blood glucose levels of hucMSC-ex-treated T2DM rats continued to decrease and were maintained at 15.49 ± 2.80 mmol/L, which did not show significant differences compared to that of the hucMSC group (16.73 ± 3.35 mmol/L). On the contrary, the blood glucose levels of control T2DM rats increased to 32.13 ± 2.60 mmol/L (Figure 1a).

DOI: 10.1021/acsnano.7b07643
ACS Nano 2018, 12, 7613−7628

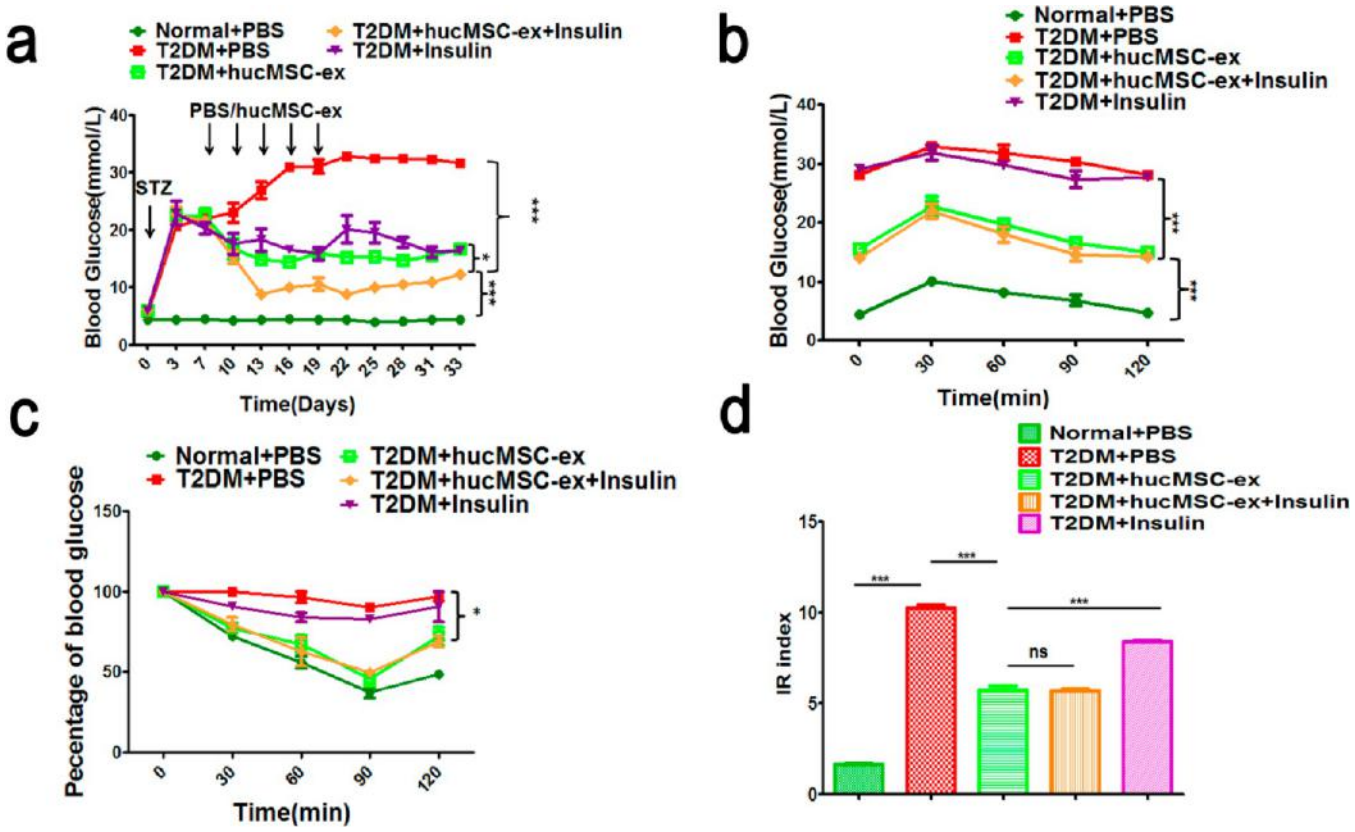

Figure 3. HucMSC-ex ameliorated the insulin resistance in T2DM rats. T2DM rats were randomly divided into four groups with PBS (0.2 mL), hucMSC-ex (10 mg/kg bw), insulin (2 IU/kg bw), and hucMSC-ex/insulin intervention; the normal group was treated with PBS as the control. (a) Blood glucose levels of each group were determined every 3 days (each group compared with T2DM + hucMSC-ex + insulin). (b) Individual glucose tolerance was assessed by oral glucose tolerant tests; fasted rats were administered 2 g of glucose/kg body weight by intragastric, and blood glucose levels were determined at 0, 30, 60, 90, and 120 min (each group compared with T2DM + hucMSC-ex + insulin). (c) Individual insulin tolerance was evaluated by intraperitoneal insulin tolerance tests by injecting 2 g of glucose/kg body weight immediately followed by insulin administration at a dose of 2 IU/kg bw; blood glucose levels were detected at 0, 30, 60, 90, and 120 min and compared to that at 0 min (each group compared with T2DM + hucMSC-ex + insulin). (d) IR index of each group, HOMA-IR index = (FBG [in mmol/L] × FINS [in units/L])/22.5. Blood glucose level of each group was detected after fasting for 3 h. Values of a−d are mean ± SE; n = 6 rats per group; *p < 0.05, **p < 0.01, ***p < 0.001 determined by (a−c) repeated measures ANOVA and (e) one-way ANOVA.

Cell therapy has been suggested as a new strategy for tissue injury repair. The therapeutic effects of MSC on diabetes have been verified in animal models and clinical patients.[13−16] However, MSC administration may have several disadvantages such as tumorigenic potential,[34] thrombosis,[35] and fever.[36] The low survival time of MSC *in vivo* may also limit their application.[8] Although gene modifications may improve the therapeutic efficiency of MSC,[37,38] it may add more risk to the clinical application. In addition, it is still controversial whether hucMSC can differentiate into functional cells such as pancreatic β-cells in the pancreas.[13,21] Thus, investigation of an alternative approach of MSC for the therapy of T2DM is needed. Paracrine actions are considered as the predominant mechanism for the roles of MSC in tissue repair.[39] Exosomes are described as the active nanocomponent that mediates the paracrine actions of their producing cells,[40,41] and we have already detected that hucMSC-ex can down-regulate blood glucose of T2DM rats. To confirm that hucMSC-ex is the main paracrine approach of hucMSC to regulate hyperglycemia, we added concentrated whole hucMSC-CM (10 mg/kg bw) and hucMSC-ex-free CM (10 mg/kg bw) to administer to T2DM rats and detected blood glucose levels in the same way as hucMSC-ex. According to the results, hucMSC-CM also could down-regulate blood glucose of T2DM rats and be maintained at 18.26 ± 4.95 mmol/L. On the contrary, hucMSC-ex-free CM could not decrease blood glucose of T2DM rats, as hucMSC-CM and the blood glucose levels increased to 29.76 ± 5.30 mmol/L. We pretreated hucMSC with noncompetitive N-SMase inhibitor GW4869[42] (5 μM), which can inhibit exosomes secretion. We detected the protein concentrations of exosomes derived from GW4869-pretreated hucMSC with a CA analysis kit, and the CD63 level by Western blot and GW4869 could temporarily inhibit exosome secretion in hucMSC for about 7 days *in vitro* (Figure S4a,b). We infused hucMSC-GW4869 into T2DM rats just as we did with hucMSC. The results of continuous blood glucose tests revealed that hucMSC-GW4869 could not decrease blood glucose of T2DM rats as fast as hucMSC could (Figure S4C), which provided more evidence that hucMSC-ex could be the substitution of hucMSC in T2DM treatment.

We administered T2DM rats with HFL1-ex as control to investigate whether hucMSC-ex had the special effect in hyperglycemia intervention. The continued blood glucose level detection showed that HFL1-ex could stabilize the blood glucose level to 27.41 ± 5.00 mmol/L but did not increase unlimitedly as the T2DM control group even though there were significant differences between the two groups (Figure

DOI: 10.1021/acsnano.7b07643
ACS Nano 2018, 12, 7613−7628

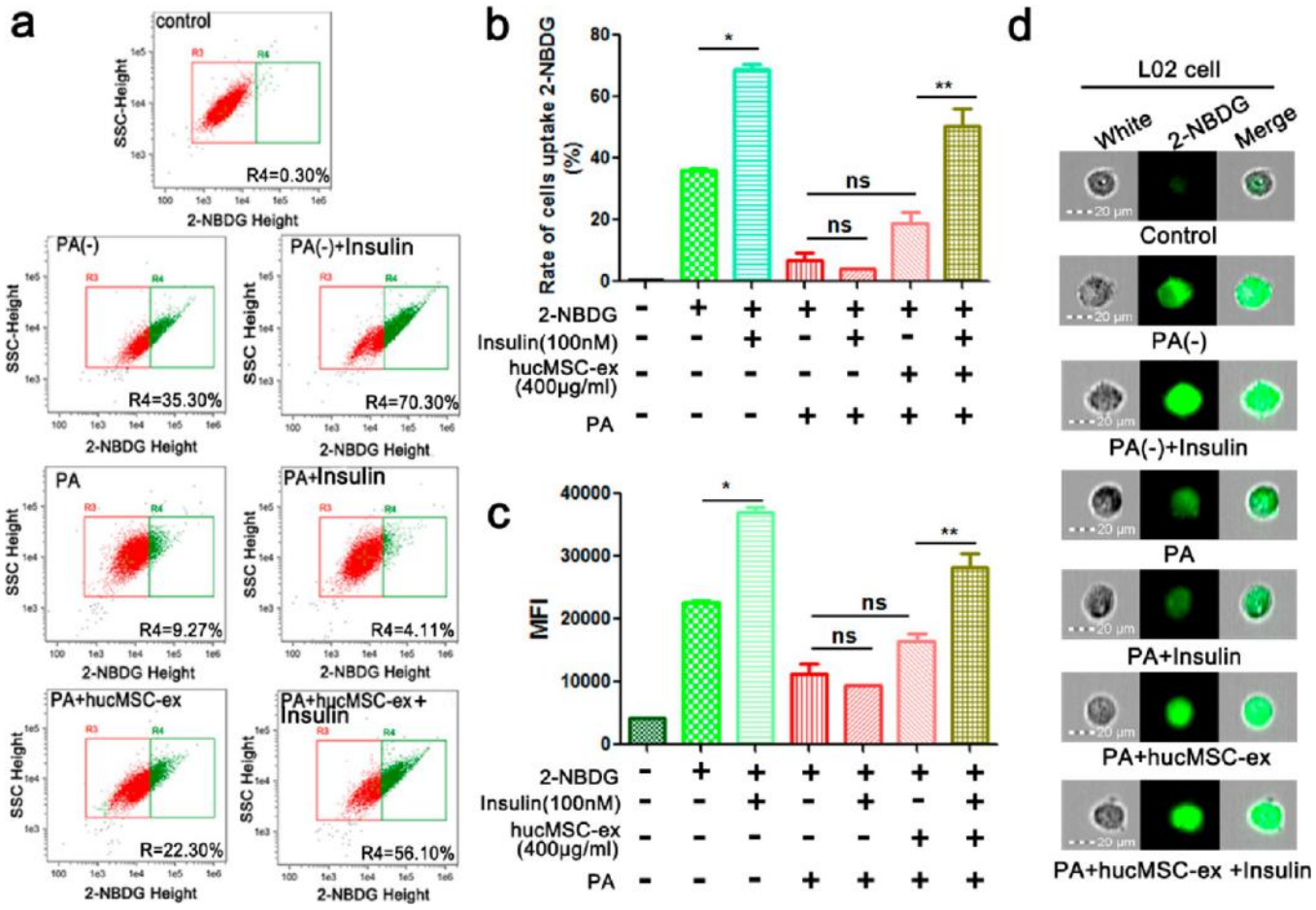

Figure 4. HucMSC-ex increased insulin sensitivity in PA-induced insulin-resistant cell model. L02 cells were divided into seven groups with PA(−), PA(−) + insulin (100 nM), PA (0.25 mM), PA + hucMSC-ex (400 μg/mL), PA + insulin, and pretreated PA + insulin + hucMSC-ex. Cells were treated with PA (PBS as control) for 24 h and washed three times by PBS and serum starved for 12 h. HucMSC-ex (PBS as control) was added and incubated for 24 h, and culture medium was removed. After being washed by PBS three times, insulin (PBS as control) was added 30 min before being incubated with 2-NBDG (1 h); cells treated with DMSO were the blank control. (a) Effect of L02 cell uptake of 2-NBDG in different groups was detected by flow sight; scatter diagrams show the fluorescence intensity distribution of the cell (*x*-axis, 2-NBDG height; *y*-axis, SSC height; wavelength = 488 nm). (b) Rate of cell uptake of 2-NBDG in different groups of L02 cells. (c) Mean fluorescence intensity of cell uptake of 2-NBDG in different groups of L02 cells. (d) Images of L02 cell uptake of 2-NBDG were taken by image streaming (wavelength = 488 nm, scale bar = 20 μm). Values of b,c are mean ± SE, *n* = 3 per group; **p* < 0.05, ***p* < 0.01 determined by one-way ANOVA.

1b). We also treated normal rats with hucMSC-ex, and no differences with the normal control were detected (Figure 1b).

In this study, we demonstrated that hucMSC-ex could decrease blood glucose level in HFD/STZ-induced T2DM rats as hucMSC and hucMSC-CM. On the contrary, exosome-depleted culture medium from hucMSC and hucMSC with impaired exosome-producing function and HFL1-ex had minimal effects in hyperglycemia intervention, suggesting that hucMSC-ex had special effects in hyperglycemia amelioration as a main component of paracrine hucMSC.

HucMSC-ex Enhanced Glucose Uptake in Myotubes and Hepatocytes *in Vitro*. Skeletal muscle and liver are essential tissues and organs for glucose metabolism. To verify the target tissue or cells of hucMSC-ex in reversing hyperglycemia of T2DM rats, we used rat L6 skeletal muscle cell (L6-myoblasts), differentiated skeletal muscle cell (L6 cell) (Figure S5a), and human L02 cells (L02 cells) as cell models to evaluate the effect of hucMSC-ex on glucose uptake. After treatment with hucMSC-ex for 24 h, the uptake of fluorescent glucose analogue 2-NBDG[43] by rat L6 cells and L02 cells was detected. The results showed that hucMSC-ex could promote the uptake of 2-NBDG into L6 cells in a concentration-dependent manner, and 400 μg/mL may be the optimal concentration (Figure 2a,b). We also treated L6 cells with HFL1-ex (400 μg/mL) and hucMSC-ex-free CM (400 μg/mL), and the results revealed that hucMSC-ex was more efficient than HFL1-ex and hucMSC-ex-free CM in stimulating 2-NBDG uptake. HFL1-ex could promote glucose uptake slightly, whereas hucMSC-ex-free CM had no effect on 2-NBDG uptake (Figure 2c). We detected 2-NBDG uptake in L6 cells treated with insulin (100 nM) and hucMSC-ex. HucMSC-ex combined with insulin led to more uptake of 2-NBDG by L6 cell than insulin or hucMSC-ex alone (Figure 2d). HucMSC-ex also increased the uptake of 2-NBDG in L02 cells (Figure 2e). These findings indicated that hucMSC-ex could promote glucose uptake in skeletal muscle cells and liver cells either alone or together with insulin.

HucMSC-ex Increased Insulin Sensitivity in T2DM Rats and Insulin-Resistant Cell Model. Peripheral insulin resistance is responsible for the pathogenesis of T2DM.[44,45]

DOI: 10.1021/acsnano.7b07643
ACS Nano 2018, 12, 7613−7628

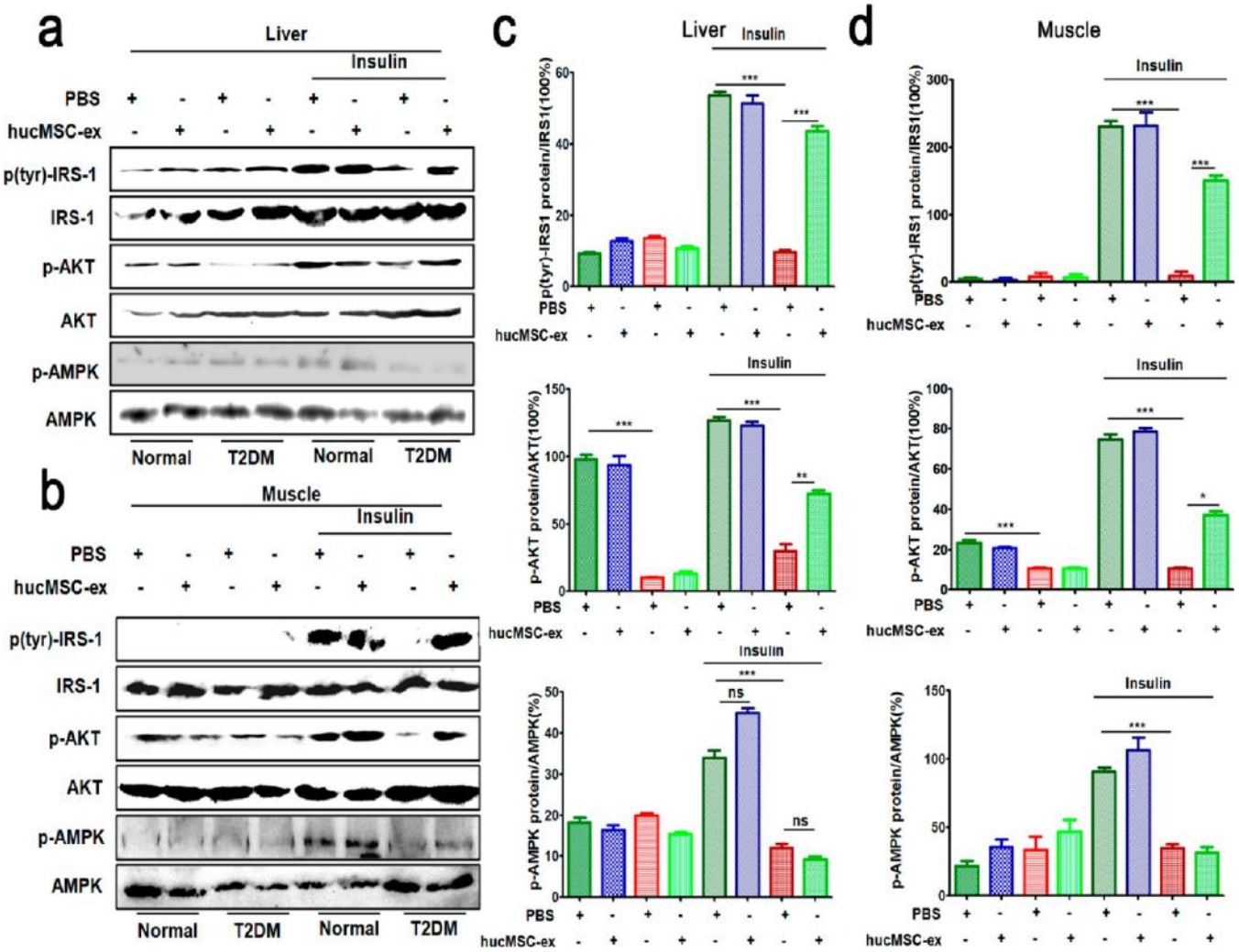

Figure 5. HucMSC-ex activated the insulin-signaling pathway in the liver and muscle of T2DM rats. Protein of liver and muscle from normal rats (treated with PBS or hucMSC-ex) and T2DM rats (treated with PBS or hucMSC-ex) was extracted. Rats in each group were administered 2 IU/kg bw insulin or PBS (as control) injection before execution. (a) Expression of p-(tyr)-IRS-1, p-AKT, and p-AMPK in the liver was detected by Western blot. (b) Expression of p-(tyr)-IRS-1, p-AKT, and p-AMPK in muscle was detected by Western blot. (c) Quantification of p-(tyr)-IRS-1, p-AKT, and p-AMPK in (a). (d) Quantification of p-(tyr)-IRS-1, p-AKT, and p-AMPK in (b). Values of c, d are mean ± SE, $n = 3$ per group; *$p < 0.05$, **$p < 0.01$, ***$p < 0.001$ determined by one-way ANOVA.

We wanted to know whether hucMSC-ex affected insulin sensitivity of T2DM rats to regulate blood glucose. We compared the blood glucose levels of T2DM rats treated with PBS, hucMSC-ex, insulin, and hucMSC-ex combined with insulin. The blood glucose level in hucMSC-ex combined with insulin group was lower than that of hucMSC-ex or insulin groups, indicating that hucMSC-ex could increase insulin sensitivity in T2DM rats (Figure 3a). We then detected the OGTTs and IPITTs levels of rats at 2 weeks after the last hucMSC-ex injection. The results of OGTTs indicated that glucose metabolism was significantly ameliorated by hucMSC-ex administration (Figure 3b). The results of IPITTs also showed that there was a significant improvement in insulin sensitivity after treated with hucMSC-ex in T2DM rats (Figure 3c). The homeostasis model assessment of insulin resistance (HOMA-IR) index in the hucMSC-ex-treated group was much lower than that in the control group, and exogenous insulin could not influence the individual insulin sensitivity (Figure 3d).

To determine whether hucMSC-ex could improve insulin sensitivity *in vitro*, we established palmitic acid (PA)-induced insulin-resistant cell models.[46] The fluorescent intensity of 2-NBDG in PA-induced insulin-resistant L02 cells was weaker than that in insulin-sensitive cells. Insulin could promote the uptake of 2-NBDG in insulin-sensitive but not insulin-resistant L02 cells (Figure S5b). The induced expression of tyrosine phosphorylation of insulin receptor substrate 1 (p(tyr)-IRS-1) by insulin was inhibited in the resistant L02 cells (Figure S5c). We then detected the effect of hucMSC-ex on the uptake of 2-NBDG in PA-induced insulin-resistant L02 cells in the presence or absence of insulin by using imaging flow cytometry. PA impaired glucose uptake of L02 cells can be partially reversed by hucMSC-ex, and this effect was more remarkable combined with insulin (Figure 4a). Both of the mean fluorescence intensity of 2-NBDG and the percentage of cells uptake of 2-NBDG in insulin-resistant cells were increased by hucMSC-ex (Figure 4b,c). Furthermore, images of L02 cells pretreated with PA had a fluorescence intensity lower than that of the non-PA group and could not be reversed by insulin

DOI: 10.1021/acsnano.7b07643
ACS Nano 2018, 12, 7613−7628

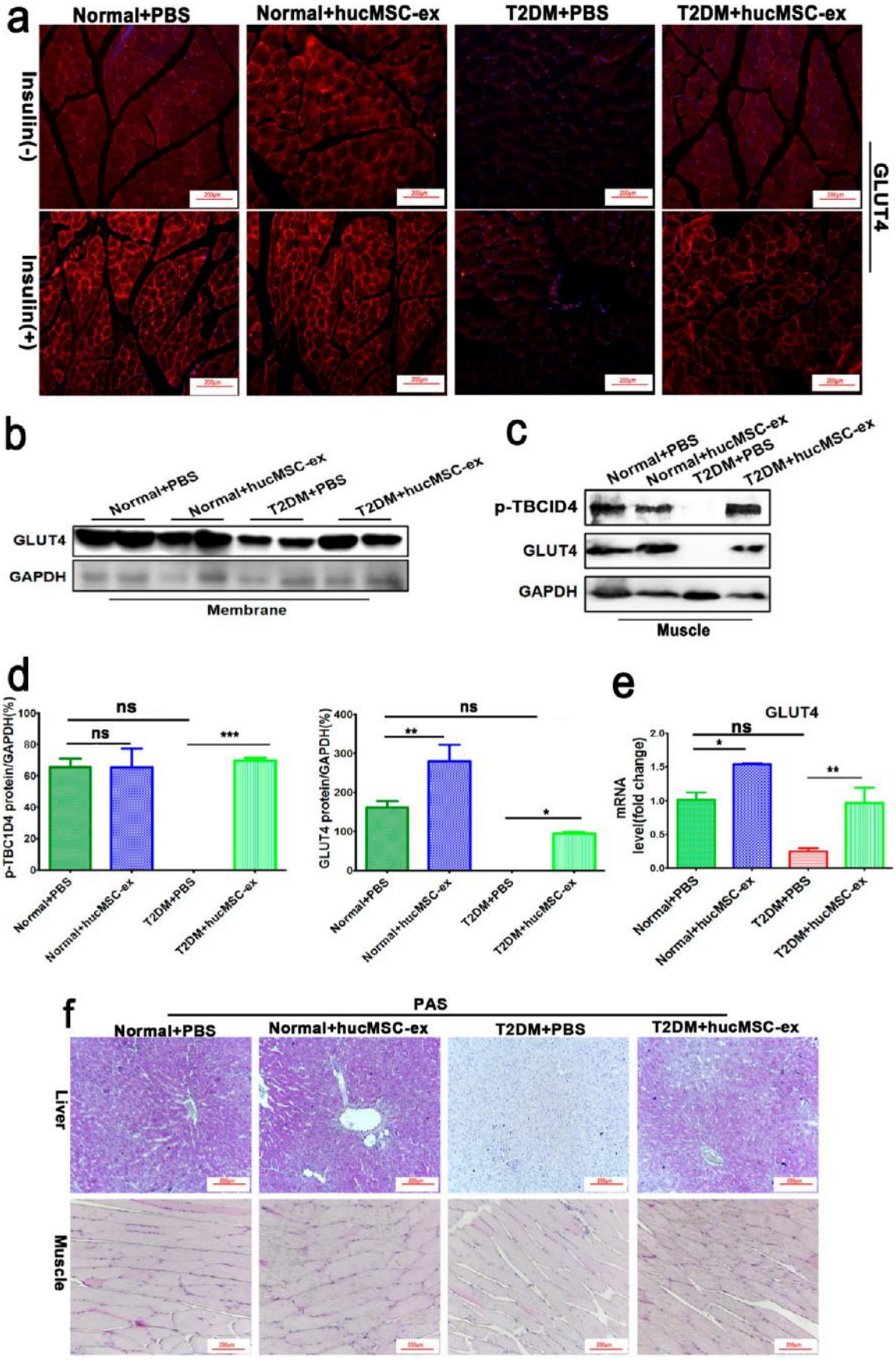

Figure 6. continued

DOI: 10.1021/acsnano.7b07643
ACS Nano 2018, 12, 7613−7628

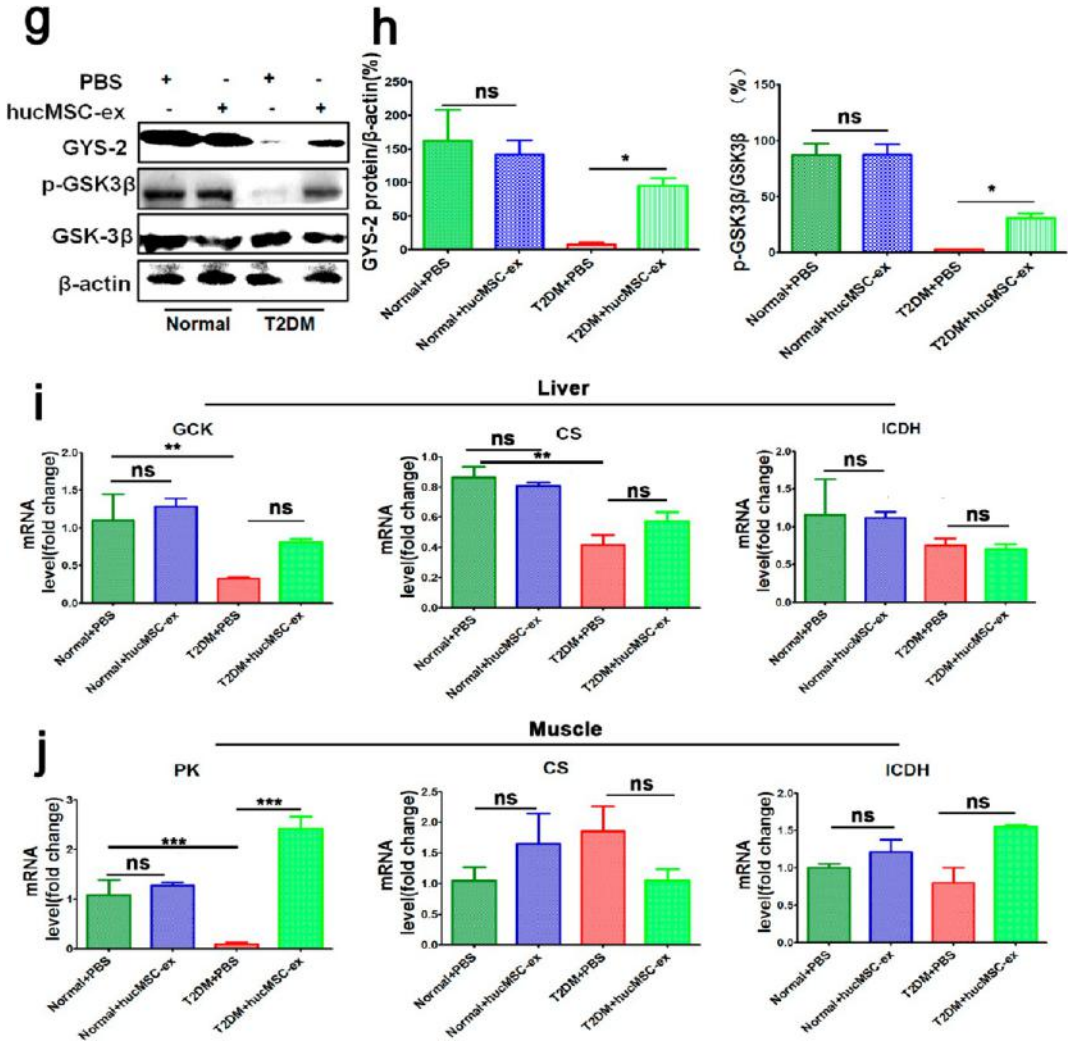

Figure 6. HucMSC-ex promoted glucose uptake and glycolysis in muscle and glycogen storage in liver in T2DM rats. (a) Muscle histology from four groups (normal group treated with PBS or hucMSC-ex, T2DM groups treated with PBS or hucMSC-ex) pretreated with PBS or insulin (2 IU/kg bw) was studied in immunofluorescence to detect the membrane translocation of GLUT4 (red); representative images of muscle sections were observed under fluorescence microscopy (scale bar = 200 μm). (b) Expression of GLUT4 relative membrane protein of muscle from rats in four groups (normal group treated with PBS or hucMSC-ex, T2DM groups treated with PBS or hucMSC-ex) pretreated with insulin was detected by Western blot. (c) Expression of p-TBC1D4 and GLUT4 of muscle from rats in four groups pretreated with insulin was detected by Western blot. (d) Quantification of p-TBC1D4 and GLUT4 in (c). (e) Expression of GLUT4 mRNA in muscle was analyzed by quantitative RT-PCR. (f) Liver and muscle histology was studied in 4 μm; representative images of periodic acid Schiff staining of liver and muscle sections were observed under light microscopy (scale bar = 200 μm). (g) Expression of p-GSK3β and glycogen synthase 2 (GYS-2) in liver was detected by Western blot. (h) Quantification of p-GSK3β and GYS-2 in (g). (i) Expression of glucokinase (GCK), citrate synthase (CS), and isocitrate dehydrogenase (ICDH) mRNA in liver was analyzed by quantitative RT-PCR. (j) Expression of pyruvate kinase (PK), CS, and ICDH mRNA in muscle was analyzed by quantitative RT-PCR. Values of b,c are mean ± SE n = 6 rats per group; *p < 0.05, **p < 0.01, ***p < 0.001 determined by one-way ANOVA.

alone but could be reversed by insulin combined with hucMSC-ex (Figure 4d). Additionally, hucMSC-ex also promoted glycogen synthesis in PA-induced insulin-resistant L02 cells, either alone or in combination with insulin (Figure S6a). These results indicated that hucMSC-ex could increase insulin sensitivity both in T2DM rats and insulin-resistant cell model.

HucMSC-ex Activated Insulin Signaling To Promote Insulin Sensitivity. IRS-1 tyrosine phosphorylation and insulin-signaling pathway activation are critically involved in glucose transport and glucose metabolism in the liver and skeletal muscle. The impaired tyrosine phosphorylation of IRS-1 and the inactivation of protein kinase B (AKT) are hallmarks of insulin resistance in T2DM.[13,47,48] To elucidate whether hucMSC-ex has the ability to activate the insulin signaling directly, we detected the expression of p(tyr)-IRS-1 and p-AKT in the liver and muscle of rats starved overnight in four groups (normal + PBS, normal + hucMSC-ex, T2DM + PBS, and T2DM + hucMSC-ex). The expression of p(tyr)-IRS-1 had no differences between normal groups or T2DM groups both in liver or muscle, and the expression of p-AKT was much lower in T2DM groups compared with that in the normal groups (Figure 5a–d). HucMSC-ex could not increase the expression of p(tyr)-IRS-1 and p-AKT directly without insulin. We then detected p(tyr)-IRS-1 and p-AKT in insulin (2 IU/kg bw) pretreated groups; expression of p(tyr)-IRS-1 and p-AKT was dramatically increased in normal groups, and no differences were detected between PBS or hucMSC-ex

DOI: 10.1021/acsnano.7b07643
ACS Nano 2018, 12, 7613–7628

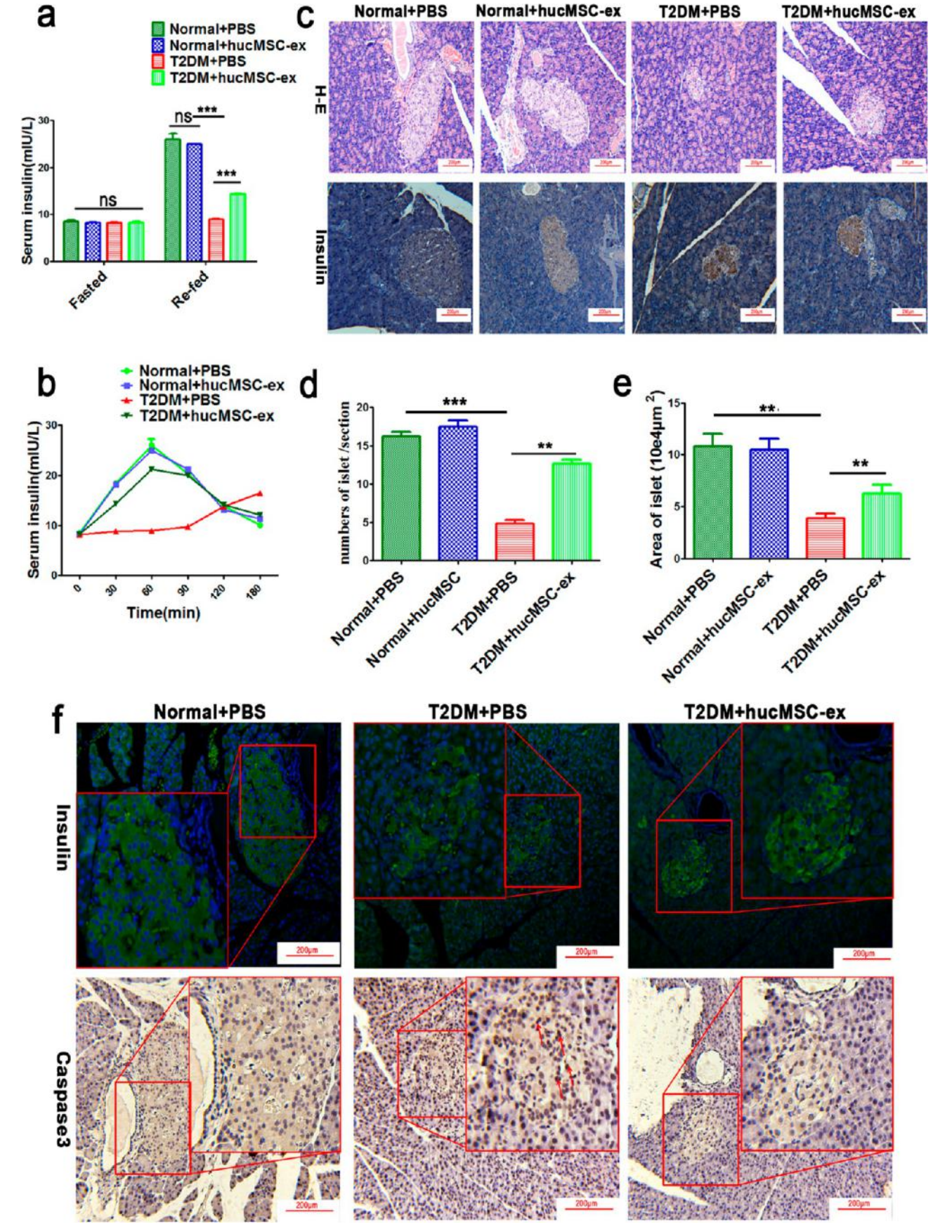

Figure 7. continued

DOI: 10.1021/acsnano.7b07643
ACS Nano 2018, 12, 7613−7628

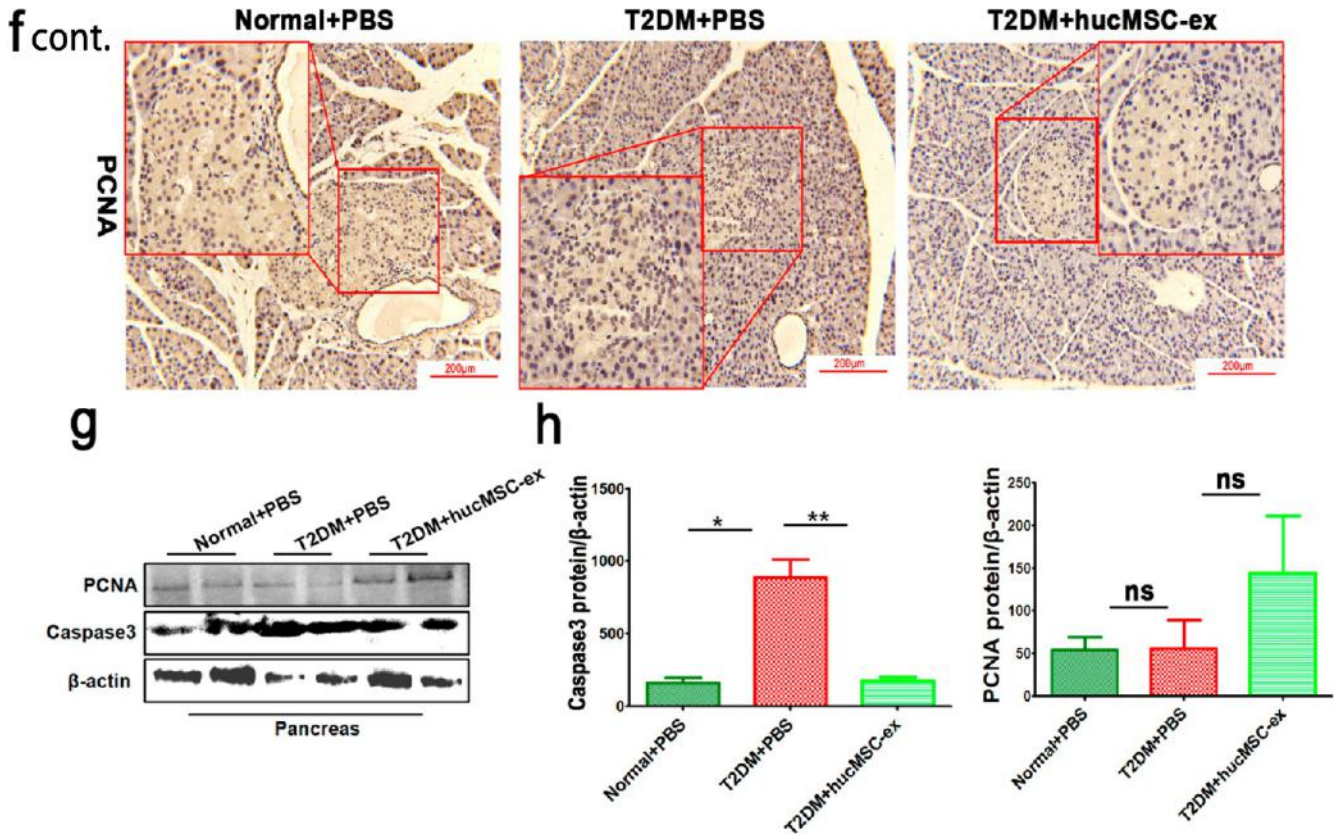

Figure 7. HucMSC-ex relieved the destructed islets in T2DM rats by inhibit STZ induced apoptosis. (a) Individual insulin levels of fasting and re-fed rats in four groups (normal group treated with PBS or hucMSC-ex, T2DM groups treated with PBS or hucMSC-ex) were evaluated by ELISA. (b) Individual insulin level in four groups was assessed by insulin release test, involving administration of 2 g of glucose/kg body weight and determination of serum insulin levels at 0, 30, 60, 120, and 180 min. (c) Morphology of pancreatic islets in four groups stained with hematoxylin/eosin (H&E), and β-cells were characterized by immunohistochemistry (IHC) staining according to the presence and distribution of insulin (yellow) (scale bar = 200 μm). (d) Amounts of pancreatic islets in four groups observed in H&E-stained sections were quantified. (e) Area of pancreatic islets in four groups observed in IHC-stained sections were quantified. (f) Serial sections of the pancreas from different groups (T2DM groups treated with PBS or hucMSC-ex, normal group treated with PBS as control) were prepared and used to detect insulin to locate β-cells in immunofluorescence (green); caspase-3 and PCNA were detected in immunohistochemical staining (brown, red arrow point) (scale bar = 200 μm). (g) Pancrease protein from animal models (T2DM groups treated with PBS or hucMSC-ex, normal group with PBS as control) was extracted, and the expression of caspase-3 and PCNA was detected with Western blot. (h) Quantification of caspase-3 and PCNA in (g). Values of a−e are mean ± SE n = 6 rats per group; *p < 0.05, **p < 0.01, ***p < 0.001 determined by one-way ANOVA.

treatment (Figure 5a−d). Insulin could increase the expression of p(tyr)-IRS-1 and p-AKT in the T2DM group treated with hucMSC-ex but not in the PBS control (Figure 5a−d). Additionally, insulin and the AMP-activated protein kinase (AMPK)-signaling pathway[43,49] are cross-linked and we would like to verify if AMPK-signaling pathways were also activated. According to the results, the activation of AMPK could only be detected in normal groups, and insulin was required; hucMSC-ex could not influence the expression of p-AMPK in normal groups or T2DM groups (Figure 5a−d). *In vitro*, hucMSC-ex could also increase the activation of p(tyr)-IRS-1 and p-AKT of PA-induced insulin-resistant L02 cells with insulin treatment (Figure S6b).

In general, chronic inflammation in tissue is the main inducement of insulin resistance, which leads to inflammatory cells secreting pro-inflammatory cytokines such as tumor necrosis factor alpha (TNF-α) or interleukin 6 (IL-6) to inhibit insulin-signaling pathway activation,[50,51] so we collected the serum of animal models in different groups and detected the level of TNF-α and IL-6. The serum level of TNF-α in hucMSC-ex-treated T2DM rats was much lower than that in the PBS control (Figure S7a), but no significant difference in serum level of IL-6 was detected between two groups (Figure S7b). These data indicated that hucMSC-ex might inhibit secretion of pro-inflammatory cytokine such as TNF-α to reverse insulin resistance in T2DM and increase the activation of the insulin/AKT-signaling pathway but not the insulin/AMPK-signaling pathway indirectly.

HucMSC-ex Promoted Glucose Uptake of Skeletal Muscles and Glycogen Storage in the Liver. Skeletal muscle and the liver play essential roles in maintaining blood glucose balance through the regulation of glucose uptake, storage, production, and consumption. STZ and HFD may dramatically decrease glucose uptake by inhibiting the expression and membrane translocation of GLUT4, which is the main glucose transporter in muscle,[13,52] and influence glycogen synthesis in the liver.[15] To investigate the effects of hucMSC-ex in glucose uptake, we detected the membrane translocation of GLUT4 by immunofluorescence in the muscles of T2DM rats treated with or without insulin before execution in different groups. HucMSC-ex-treated T2DM rats showed more GLUT4 translocation on the membrane of

DOI: 10.1021/acsnano.7b07643
ACS Nano 2018, 12, 7613−7628

muscle than did the PBS control (Figure 6a), and insulin was required. We also detected expression of GLUT4-related protein in the membrane of muscle by Western blot after insulin stimulation. HucMSC-ex-treated T2DM groups had more GLUT4 on the membrane than did the PBS control (Figure 6b). The expression of total GLUT4 in T2DM groups was decreased; hucMSC-ex could up-regulate it in both protein and gene level with or without insulin pretreatment in the normal group or the T2DM group (Figure 6a,c−e). However, hucMSC-ex could not significantly increase membrane translocation of GLUT4 in the normal group (Figure 6a,b), which means that hucMSC-ex might influence the expression of GLUT4, but the membrane translocation of GLUT4 still depends on the insulin-signaling pathway. In insulin-treated T2DM groups, hucMSC-ex up-regulated the phosphorylation of TBC1D4 (AS160), which is an important protein in the regulation of GLUT4 translocation and can be activated by the insulin/AKT-signaling pathway[53] (Figure 6c,d). These results indicated that hucMSC-ex promoted muscle uptake of glucose depending on the reversal of insulin resistance and increased GLUT4 expression of T2DM rats.

Glucose also can be taken up by the liver but in an insulin-dependedent way and relies on glucose-sensitive transporter GLUT2,[54] which can be increased by STZ. We detected the expression of hepatic GLUT2 with immunohistochemical staining and Western blot. Normal groups and T2DM rats treated with hucMSC-ex had lower translocation of GLUT2 in the membrane (Figure S8), which indicated that the blood glucose level in hucMSC-ex-treated group was lower than that in the T2DM control.

To verify the effect of hucMSC-ex in regulating glucose metabolism of T2DM rats, we determined the level of glycogen deposits in the liver and muscle sections by using periodic acid Schiff staining. The hucMSC-ex-treated T2DM group showed more glycogen accumulation in the liver (Figure 6f). The expression of glycogen synthesis-related protein p-GSK3β and glycogen synthase in the liver was detected by Western blot, and hucMSC-ex-treated T2DM rats had an expression of p-GSK3β and glycogen synthase (Figure 6g,h) higher than those in the control group. HucMSC-ex could not change the glycogen synthesis in the normal group (Figure 6f−h). *In vitro*, the higher levels of p-GSK3β and glycogen synthase (Figure S6b) were also verified in insulin-resistant cell model L02 either alone or in combination with insulin. However, no differences of glycogen level between normal groups and T2DM groups or PBS control and hucMSC-ex-treated groups were observed in muscle (Figure 6f). We next assessed whether hucMSC-ex treatment influenced the expression of enzymes that were involved in glucose metabolism such as citrate synthase (CS), isocitrate dehydrogenase (ICDH), glucokinase (GCK), or PK. In the liver, PK could barely be detected; the levels of GCK and CS in T2DM groups were lower than those in normal groups, and we had no evidence to prove that hucMSC-ex can influence their expression (Figure 6i). The expression of PK was greatly decreased in the skeletal muscle of T2DM rats but was up-regulated by hucMSC-ex treatment, which means hucMSC-ex might intervene in the glycolysis of muscle of T2DM rats. Minimal GCK could be detected in muscle, and the expression of CS and ICDH showed no significant difference between normal groups and T2DM groups with or without hucMSC-ex treatment (Figure 6j). These results indicated that hucMSC-ex activated the insulin signaling to improve glycogen synthesis in the T2DM rats, restore glucose homeostasis in the liver, but promote glucose uptake and glycolysis in skeletal muscle.

HucMSC-ex Promoted Insulin Secretion and Islet Regeneration by Inhibiting STZ-Induced Cell Apoptosis. In T2DM, the release of insulin by pancreatic β-cells is impaired.[1,4] HFD/STZ-induced T2DM rats have destroyed pancreatic islets, which leads to impaired insulin production. In our study, we indicated that hucMSC-ex reversed impaired insulin-secreting function of re-fed T2DM rats by serum insulin level detection and insulin-releasing tests (IRTs) (Figure 7a,b). The results of H&E staining and IHC staining for pancreatic tissue sections revealed that the count and area of islets in the hucMSC-ex-treated T2DM group were higher than that in the T2DM control (Figure 7c−e). HucMSC-ex could not influence the insulin secretion, islet structure, or numbers in normal groups (Figure 7a−e). We also detected the islet structure of low-dose STZ injected pancreatic damage of SD rats with early (7 days) or later (14 days) hucMSC-ex (10 mg/kg bw, signal dose) infusion; there was no obvious difference in area between early and later hucMSC-ex infusion, but we observed that the structure of the islet with early hucMSC-ex infusion was more uniform than the later one, and later hucMSC-ex infusion or without hucMSC-ex treatment had more vacuolar degeneration (Figure S9a). These results indicated that hucMSC-ex could relieve STZ-induced pancreatic damage in T2DM rats by protecting against pancreatic islet destruction in the early phase. To figure out how hucMSC-ex restored the islets, we executed the T2DM rats 1 week after a single dose hucMSC-ex treatment. We detected the proliferation-related protein proliferating cell nuclear antigen (PCNA) and apoptosis-related indicator caspase-3 in pancreas serial sections. There was no difference of PCNA between the normal group and T2DM groups, but caspase-3 was up-regulated in T2DM rats, and hucMSC-ex could decrease it (Figure 7f). We also detected the pancreas protein from three groups (normal + PBS, T2DM + PBS, T2DM + hucMSC-ex) with Western blot; T2DM groups had an expression of caspase-3 much higher than that of other groups, and the hucMSC-ex-treated T2DM group had no difference from the normal group (Figure 7g,h). The level of PCNA in three groups had no significant differences (Figure 7g,h). These data verified that hucMSC-ex promoted insulin secretion and islet regeneration by inhibiting STZ-induced cell apoptosis.

Exosomes have proven that they can be an emerging source of biomaterials in impaired tissue repair.[29−32] Exosomes from cardiomyocytes and adipose tissues have been reported to regulate glucose metabolism.[24,25] Neutral ceramidase-enriched exosomes could not only inhibit PA-induced cell apoptosis but also rescue PA-induced insulin resistance.[46,55] MiR-containing exosomes secreted by adipose tissue macrophage (ATM) in obese mice can cause glucose intolerance and insulin resistance in lean mice. On the contrary, ATM-ex obtained from lean mice improved glucose tolerance and insulin sensitivity when administered to obese recipients.[51] The therapeutic effects of exosomes on the complications of diabetes mellitus has also been reported. For example, exosomes from nondiabetic plasma could repair ischemic heart disease in T2DM by activating cardioprotective signaling.[56] Exosomes secreted from human urinary stem cells could ameliorate diabetic kidney disease by reducing podocyte apoptosis and enhancing glomerular endothelial cell proliferation.[57] Exosomes derived from MSC transported miR-133a to promote axonal

DOI: 10.1021/acsnano.7b07643
ACS Nano 2018, 12, 7613−7628

remodeling and neuronal outgrowth in diabetes-induced central nervous system damage.[58] In addition, exosomes derived from MSC could deliver Fas shRNA and miR-375 antagonist to modulate immune response and improve islet transplantation.[59] These studies suggest that exosomes derived from healthy tissues or cells can be used as a potential tool for therapeutic intervention.

In our study, hucMSC-ex decreased blood glucose levels in HFD/STZ-induced T2DM rats just like hucMSC or hucMSC-CM, whereas exosome-depleted culture medium from hucMSC and exosome-producing impaired hucMSC had no effects. These results indicated that exosomes were one of the key factors for the therapeutic effects of hucMSC on hyperglycemia. HucMSC-ex could improve peripheral insulin sensitivity and increase the activation of IRS-1 (tyrosine site), AKT, and downstream signaling pathways in T2DM indirectly. This progress was possibly caused by hucMSC-ex decreasing the serum pro-inflammatory cytokine TNF-α, which plays an important role in the development and progression of individual insulin resistance. In muscle, hucMSC-ex promoted the expression of GLUT4 in both physiological status and T2DM but only increased the membrane translocation of GLUT4 in T2DM groups. Additionally, hucMSC-ex treatment protected the STZ-induced destruction of islets in T2DM rats by inhibiting β-cell apoptosis. These findings indicated that hucMSC-ex might regulate glucose metabolism of T2DM, not only relying on a single approach or single component but also depending on multiple components. We analyzed the components by LC/MS-MS and found that hucMSC-ex contained thousands of proteins, and most of them were different with proteins from HFL1-ex. These proteins take part in many signaling pathways, especially the metabolism-related insulin pathway, pyruvate metabolism, and pentose phosphate pathways. Our previous work also found that hucMSC-ex could deliver glutathione peroxidase 1 to improve hepatic oxidant injury recovery[29] and Wnt4 to mediate the β-catenin-signaling pathway in cutaneous wound healing repair,[10] which indicated that hucMSC-ex proteins might also be the efficient component in T2DM intervention. Exosomes' characteristics ensure that they can be internalized efficiently. On the basis of the previous work of Sun[26] and Yameen,[27] in our research, we discovered the biodistribution of hucMSC-ex in T2DM rats and normal rats 24 h after infusion, where most of the hucMSC-ex spread to the liver, lung, pancreas, spleen, and kidney (Figure S10a). HucMSC can be easily derived from umbilical cord, and the donation of the umbilical cord is enough,[60] which can be a stable source of exosomes, hucMSC-ex can be purified with 30% sucrose/D_2O density gradient centrifugation, which guarantees the quantity and purity,[10,61] and these features provided the basis for the application of hucMSC-ex in T2DM and indicated that hucMSCs-ex could be a potential nanomedicine for type 2 diabetes mellitus intervention.

Given the safety evaluation of hucMSC-ex, relevant research has been carried out. We treated healthy rabbits, guinea pigs, and rats with hucMSC-ex,[62] and no evidence proved that hucMSC-ex could lead to tumorigenesis. There was no obvious hemolysis, systemic anaphylaxis, or liver and renal toxicity in the different kinds of animals.[62] We also detected the body weight and liver and renal function of rats in hucMSC-ex or PBS-treated normal or T2DM rats 2 months after the last infusion of hucMSC-ex to figure out whether hucMSC-ex changes the function of healthy tissues in T2DM or normal rats. HucMSC-ex infusion did not influence the weight and liver or renal function of normal rats compared with PBS control (Figure S11). In T2DM rats, the body weight of hucMSC-ex-treated T2DM rats was greater than that of the control group, which indicated that hucMSC-ex treatment could relieve the rapid emaciation of T2DM rats (Figure S11a). No significant differences of alanine aminotransferase (Figure S11b), alanine aminotransferase/aminotransferase (ALT/AST) (Figure S11c), blood urea nitrogen (BUN) (Figure S11d), or creatinine (CREA) (Figure S11e) were found between hucMSC-ex-treated T2DM groups and normal groups. These data indicated that hucMSC-ex did not significantly damage healthy tissues, which provided partial evidence for the safety of future clinic applications. For clinic transformation of hucMSC-ex, other elements are necessary, such as development of more standardized methods for purifying the therapeutic level of exosomes to stabilize curative effects, using hucMSC-ex in combination with proper antidiabetic drugs, or modifying hucMSC-ex to further improve its efficacy. These further studies can be carried out based on our study.

CONCLUSION

In conclusion, we reported for the first time that hucMSC-ex could effectively alleviate hyperglycemia in HFD/STZ-induced T2DM rats by promoting insulin sensitivity, increasing glucose uptake and metabolism in peripheral tissues, and protecting pancreatic islets from damage by inhibiting STZ-induced β-cell apoptosis. Our study provided a basis for the application of hucMSC-ex as another approach of the therapy for type 2 diabetes mellitus.

METHODS

All experimental protocols were approved by the Medical Ethics Committee of Jiangsu University (2012258).

Cell Culture. HucMSC was isolated as previously described.[60] The cells in passage 3−4 were used for experiments. For exosomes secretion inhibition, hucMSC was pretreated with the noncompetitive N-SMase inhibitor GW4869 (Santa Cruz Biotechnology, 5 μM) for 24 h. Human lung fibroblast 1 (HFL1), rat skeletal muscle cells (L6-myoblast), and human L02 cells (L02 cells) were purchased from the Cell Bank of Chinese Academy of Sciences and maintained in a high-glucose Dulbecco's modified Eagle medium (DMEM) or RPMI-1640 supplemented with 10% fetal bovine serum (Gibco, Grand Island, USA) at 37 °C with 5% CO_2. L6-myoblasts were plated in 6-well plates and induced to differentiate into myotubes (L6 cells) as previously described.[63] L02 cells were incubated with palmitic acid (Sigma-Aldrich, 0.25 mM) for 24 h to establish an insulin-resistant cell model.[46]

Exosome Purification and Characterization. HucMSC-ex and HFL1-ex were purified from cell culture supernatant as previously described.[30−32] The exosome-depleted supernatant (hucMSC-ex-free CM) was passed through a 0.22 μm filter and stored at −70 °C for future use. The protein contents of the isolated exosomes and hucMSC-ex-free CM were determined by using a BCA protein assay kit (CWBIO). The final concentration of hucMSC-ex for *in vitro* use was 400 μg/mL and 10 mg/kg for *in vivo* studies. Exosomal markers CD9 and CD81 were determined by using Western blot. The morphology and size distribution of exosomes were identified by using transmission electron microscopy (FEI Tecnai 12, Philips, The Netherlands) and nanosight tracking analysis (NanoSight, Amesbury, UK).[32]

Type 2 Diabetes Mellitus Animal Model. Eight week old male Sprague−Dawley (SD) rats (200−250 g) were purchased from the Animal Centre of Chinese Academy of Sciences (Shanghai, China). The rats were housed with a 12/12 h light/dark cycle at an ambient

DOI: 10.1021/acsnano.7b07643
ACS Nano 2018, 12, 7613−7628

temperature of 22−25 °C for 5 days. The rats were fed with 45% HFD for 5 weeks. After being fasted for 12 h with free access to water, HFD fed rats were injected with STZ (35 mg/kg in 0.1 M citrate-buffered saline, pH 4.5) *via* tail vein to induce T2DM. STZ-treated rats were kept on the high-fat diet for another week and then subjected to 12 h of fasting before the blood glucose test. The rats showed fasting glucose levels of more than 16.7 mmol/L, which were considered to be T2DM rats.[14,33] For the islet impairment study, the rats were injected with STZ (35 mg/kg in 0.1 M citrate-buffered saline, pH 4.5) *via* tail vein 7 days before hucMSC-ex treatment, which demonstrated the effect of hucMSC-ex on STZ-induced β-cell impairment. Normal rats were fed normal diets.

HucMSC and HucMSC-ex Administration. T2DM rats were divided into nine groups (n = 6/group): PBS, hucMSC-ex, hucMSC, hucMSC-GW4869, hucMSC-ex-free CM, hucMSC-CM, HFL1-ex, insulin, hucMSC-ex combined with insulin. HucMSC (3×10^6) pretreated with or without GW4869 was suspended in 0.2 mL of PBS and injected into T2DM rats *via* tail vein at 7, 13, and 19 days after STZ injection. HucMSC-ex, HFL1-ex, hucMSC-CM, and hucMSC-ex-free CM in 0.2 mL of PBS (10 mg/kg bw) were injected into rats *via* tail vein every 3 days for five cycles. The rats in the insulin group were given 2 IU/kg/day of insulin. The rats in hucMSC-ex combined with insulin were administered hucMSC-ex (10 mg/kg bw) every 3 days and also given 2 IU/kg/day of insulin. Normal groups were divided into two groups: one group infused with 0.2 mL of PBS, and the other one infused with a concentration of proteins the same as that of hucMSC-ex (see supplementary Table S1 for more detailed experiment procedure). For islet impairment study, the 8 week old male SD rats were injected with STZ (35 mg/kg) and then treated with hucMSC-ex (10 mg/kg bw) in 0.2 mL of PBS *via* tail vein at an early phase (7 days after STZ injection) and late phase (14 days after STZ injection) of experiment and executed 28 days after STZ injection.

Location of HucMSC-ex *in Vivo* and *in Vitro*. *In vivo*, hucMSC-ex (10 mg/kg bw in 200 μL) was stained with fluorochrome DiR (10 μM, Themo Fisher, USA) and infused into T2DM rats or normal rats. Twenty-four hours later, we took the lung, liver, kidney, and spleen of the rats, and the location of hucMSC-ex *in vivo* was detected *via* an IVIS Lumina LT Series III (PerkinElmer, USA) (wavelength = 720 nm).[64]

Serological Analysis. One week after STZ injection, fasted and re-fed blood glucose levels, OGTTs, IPITTs, and IRTs were performed to confirm the establishment of the T2DM rat model. Two weeks after the last infusion of hucMSC-ex, OGTTs, serum insulin levels, IPITTs, IRTs, serum IL-6 levels, and serum TNFα levels were obtained to determine the effect of infused hucMSC-ex. The rats were starved for 3 h before the measurement of blood glucose levels. Tail capillary blood glucose levels were monitored with a gluco-meter ACCU-CHEKA performa (Roche Diagnostics GmbH, Mannheim, Germany). Serum insulin levels were measured by using an enzyme-linked immunosorbent assay (ELISA) (Millipore, Billerica, MA, USA); serum IL-6 and TNFα levels were measured by using ELISA (Excel, China) according to the manufacturer's protocols. For OGTTs, the rats were fasted overnight and intragastric administered glucose (2 g/kg bw), and the blood glucose levels were detected at 0, 30, 60, 90, and 120 min after administration. IPITTs were done by injecting glucose (2 g/kg bw) into rats intraperitoneally followed by administration of insulin (2 IU/kg bw) immediately, and the blood glucose levels were detected at 0, 30, 60, 90, and 120 min after administration. For IRTs, the rats were intragastric administerd glucose (2 g/kg bw), and the serum insulin levels were detected at 0, 30, 60, 90, 120, and 180 min after administration. Two months after the last infusion of hucMSC-ex, the rats were starved for 12 h and serum AST, ALT, ALP, BUN, and CREA were detected.

Histological Analysis. The liver, muscle, and pancreas tissues were fixed in 4% paraformaldehyde, gradually dehydrated, embedded in paraffin, cut into 4 μm sections, and subjected for hematoxylin/eosin staining. Periodic acid Schiff stain was performed according to the manufacturer's protocols (Jkchem, China) on liver and muscle sections. Immunohistochemical staining was performed according to the manufacturer's protocols (Boster, China). Liver sections were incubated with rabbit anti-rat GLUT2 (1:100, Proteintech, USA). Pancreas sections were incubated with rabbit anti-rat PCNA antibody (1:1000, CST, USA) and rabbit anti-rat caspase-3 antibody (1:100, bioworld, USA) at 4 °C overnight. For immunohistofluorescence, muscle secions were incubated with rabbit anti-rat GLUT4 antibody (1:100, SAB, USA), and pancreas sections were incubated with rabbit anti-rat insulin antibody (1:100, Bioworld, USA) at 4 °C overnight. The sections were then washed and incubated with Alexa Fluor 555 conjugated donkey anti-rabbit IgG or FITC-conjugated goat anti-rabbit IgG (Invitrogen) for 1 h. Subsequently, sections were stained with Hoechst 33342 at 0.5 μg/mL before being observed under a microscope.

Glucose Uptake Assay. Glucose uptake in L6 cells and L02 cells was analyzed by 2-NBDG method (Life Technologies, USA).[43] Briefly, the differentiated L6 cells and L02 cells seeded in 6-well plates were starved for 12 h and treated with different doses of hucMSC-ex (0, 50, 100, 200, 400 μg/mL) in serum-free medium for 24 h. The medium was discarded, and the cells were washed with PBS for three times. We used insulin (100 nM) or not to verify the effect of hucMSC-ex in regulating insulin sensitivity (incubated for 30 min). Then, 2-NBDG (100 μM) was added into the cells. After 1 h, the cells were collected and subjected to flow cytometric analysis (BD FACS Calibur) and microscopic observation (Nikon, Tokyo, Japan). HLF1-ex and hucMSC-ex-free CM were used to demonstrate the specific effect of hucMSC-ex on 2-NBDG uptake.

Western Blot. Total protein was extracted from tissues and cells by using RIPA lysis buffer. For insulin-signaling pathway analysis, animals were starved overnight and treated with insulin (2 IU/kg bw) or PBS (control). Cell membrane protein was prepared from skeletal muscle and liver by using a Proteo-Prep membrane extraction kit (Beyotime Biotechnology, China). The protein concentration was determined by using a BCA protein assay kit. Equal amounts of protein were separated on 12% SDS-PAGE gel and then transferred onto polyvinylidene fluoride membranes. After blockade with 5% skim milk for 1 h, the membranes were incubated with primary and HRP-conjugated secondary antibodies and detected using an ECL detection system (Amersham Pharmacia Biotech, Little Chalfont, UK). The primary antibodies were as follows: CD9 (1:500; Bioworld, USA), CD81 (1:500, Abcam, UK), GLUT4 (1:400, SAB, USA), GLUT2 (1:400, Proteintech, USA), AKT (1:500, CST, USA), Phospho-Akt (1:500, CST, USA), IRS-1 (1:200, SAB, USA), IRS-1 (phospho-tyr896) (1:500, SAB, USA), GSK-3β (1:500, SAB, USA), GSK3β (phospho-Ser9) (1:500, SAB, USA), AMPK (1:500; Bioworld, USA), p-AMPK (1:500, Bioworld, USA), glycogen synthase2 (1:500, Bioworld, USA), PCNA (1:5000, CST, USA), caspase-3 (1:400, Bioworld, USA), p-TBC1D4 (1:400, Bioworld, USA), GAPDH (1:2000, CWBIO, China), β-actin (1:2000, CWBIO, China). The secondary antibodies were HRP-conjugated goat anti-rabbit and goat anti-mouse antibodies (1:2000, CWBIO, China).

QRT-PCR. Total RNA was extracted from the skeletal muscle, liver, L6 cells, and L02 cells. The expression levels of target genes were determined by using reverse and real-time quantitative PCR. β-Actin was used as the internal control. The primers were provided by Invitrogen (Shanghai, China), and their sequences are shown in supplementary Table S2.

Statistical Analysis. All the data are shown as mean ± standard deviation. The statistically significant differences between groups were assessed by two-way ANOVA with Bonferroni comparisons, repeated measures ANOVA, or unpaired t test using Prism software (GraphPad, San Diego, USA). A value of $p < 0.05$ was considered significant.

ASSOCIATED CONTENT

Supporting Information

The Supporting Information is available free of charge on the ACS Publications website at DOI: 10.1021/acsnano.7b07643.

Figures S1−S11; supplementary Tables S1 and S2 (PDF)

DOI: 10.1021/acsnano.7b07643
ACS Nano 2018, 12, 7613−7628

AUTHOR INFORMATION

Corresponding Authors

*Tel: +86 511 85038215. Fax: +86 511 85038483. E-mail: icls@ujs.edu.cn.

*Tel: +86 511 85038334. Fax: +8651185038483. E-mail: lstmmmlst@163.com.

ORCID

Hui Qian: 0000-0003-3054-575X

Author Contributions

§Y.S., H.S., and S.Y. contributed equally to this work.

Notes

The authors declare no competing financial interest.

ACKNOWLEDGMENTS

This work was supported by the National Natural Science Foundation of China (Grant Nos. 81572075, 81670549, and 81670502), the Natural Science Foundation of Jiangsu Province (Grant Nos. BE2016717, BE2015667), the Innovation Project for Graduate Student Research of Jiangsu Province (Grant No. KYZZ16_0342), the opening project of the Key Laboratory of Embryo Molecular Biology, Ministry of Health of China, and Shanghai Key Laboratory of Embryo and Reproduction Engineering (Grant No. KF201601), and Project Funded by the Priority Academic Program Development of Jiangsu Higher Education Institutions.

REFERENCES

(1) World Health Organization. Global Report on Diabetes. *Working Papers*, 2016.

(2) Nyenwe, E. A.; Jerkins, T. W.; Umpierrez, G. E.; Kitabchi, A. E. Management of Type 2 Diabetes: Evolving Strategies for the Treatment of Patients with Type 2 Diabetes. *Metabolism* **2011**, *60*, 1−23.

(3) Holz, G. G., IV; Kiihtreiber, W. M.; Habener, J. F. Pancreatic Beta-Cells Are Rendered Glucose-Competent by the Insulinotropic Hormone Glucagon-Like Peptide-1. *Nature* **1993**, *361*, 362−365.

(4) Aburmeileh, N. M. E.; Husseini, A.; Capewell, S.; O'Flaherty, M. Preventing Type 2 Diabetes among Palestinians: Comparing Five Future Policy Scenarios. *BMJ. Open.* **2013**, *3*, e003558.

(5) Ryan, E. A.; Paty, B. W.; Senior, P. A.; Bigam, D.; Alfadhli, E.; Kneteman, N. M.; Lakey, J. R. T.; Shapiro, A. M. J. Five Year Follow-Up After Clinical Islet Transplantation. *Diabetes* **2005**, *54*, 2060−2069.

(6) Xv, J.; Ming, Q.; Wang, X.; Zhang, W.; Zheng, L.; Wang, S.; Li, Y.; Li, L. Mesenchymal Stem Cells Moderate Immune Response of Type 1 Diabetes. *Cell Tissue Res.* **2017**, *368*, 239−248.

(7) Gruessner, R. W.; Gruessner, A. C. The Current State of Pancreas Transplantation. *Nat. Rev. Endocrinol.* **2013**, *9*, 555−562.

(8) Ankrum, J.; Karp, J. M. Mesenchymal Stem Cell Therapy: Two Steps Forward, One Step Back. *Trends Mol. Med.* **2010**, *16*, 203−209.

(9) Wang, Y. J.; Yan, J.; Zou, X. L.; Guo, K. J.; Zhao, Y.; Meng, C. Y.; Yin, F.; Guo, L. Bone Marrow Mesenchymal Stem Cells Repair Cadmium-Induced Rat Testis Injury by Inhibiting Mitochondrial Apoptosis. *Chem.Biol. Interact.* **2017**, *271*, 39−47.

(10) Zhang, B.; Wang, M.; Gong, A.; Zhang, X.; Wu, X.; Zhu, Y.; Shi, H.; Wu, L.; Zhu, W.; Qian, H.; Xu, W. HucMSC-exosome Mediated-Wnt4 Signaling Is Required for Cutaneous Wound Healing. *Stem Cells* **2015**, *33*, 2158−2168.

(11) Shi, H.; Xu, X.; Zhang, B.; Xu, J.; Pan, Z.; Gong, A.; Zhang, X.; Li, R.; Sun, Y.; Yan, Y.; Mao, F.; Qian, H.; Xu, W. 3, 3′-Diindolylmethane Stimulates Exosomal Wnt11 Autocrine Signaling in Human Umbilical Cord Mesenchymal Stem Cells to Enhance Wound Healing. *Theranostics* **2017**, *7*, 1674−1688.

(12) Trinh, N. T.; Yamashita, T.; Ohneda, K.; Kimura, K.; Salazar, G.; Sato, F.; Ohneda, O. Increased Expression of Egr-1 in Diabetic Human Adipose Tissue-Derived Mesenchymal Stem Cells Reduces Their Wound Healing Capacity. *Stem Cells Dev.* **2016**, *25*, 760−773.

(13) Si, Y.; Zhao, Y.; Hao, H.; Liu, J.; Guo, Y.; Mu, Y.; Shen, J.; Cheng, Y.; Fu, X.; Han, W. Infusion of Mesenchymal Stem Cells Ameliorates Hyperglycemia in Type 2 Diabetic Rats Identification of a Novel Role in Improving Insulin Sensitivity. *Diabetes* **2012**, *61*, 1616−1625.

(14) Hao, H.; Liu, J.; Shen, J.; Zhao, Y.; Liu, H.; Hou, Q.; Tong, C.; Ti, D.; Dong, L.; Cheng, Y.; Mu, Y.; Liu, J.; Fu, X.; Han, W. Multiple Intravenous Infusions of Bone Marrow Mesenchymal Stem Cells Reverse Hyperglycemia in Experimental Type 2 Diabetes Rats. *Biochem. Biophys. Res. Commun.* **2013**, *436*, 418−423.

(15) Xie, M.; Hao, J.; Cheng, Y.; Xie, Z. Y.; Yin, Y.; Zhang, Q.; Gao, J.; Liu, H.; Mu, Y.; Han, W. Adipose-Derived Mesenchymal Stem Cells Ameliorate Hyperglycemia through Regulating Hepatic Glucose Metabolism in Type 2 Diabetic Rats. *Biochem. Biophys. Res. Commun.* **2017**, *483*, 435−441.

(16) Guan, L.; Guan, H.; Li, H.; Ren, C.; Liu, L.; Chu, J.; Dai, L. Therapeutic Efficacy of Umbilical Cord-Derived Mesenchymal Stem Cells in Patients with Type 2 Diabetes. *Exp. Ther. Med.* **2015**, *9*, 1623−1630.

(17) Li, H.; Jiang, F.; Shi, P.; Zhang, T.; Liu, X.; Lin, X.; San, Z.; Pang, X. *In Vitro* Reprogramming of Rat Bm-MSCs into Pancreatic Endocrine-Like Cells. *In Vitro Cell. Dev. Biol.: Anim.* **2017**, *53*, 157−166.

(18) Phuc, V. P.; Phuoc, T. M. N.; Anh, T. Q. N.; Vuong, M. P.; Anh, N. T. B.; Loan, T. T. D. Improved Differentiation of Umbilical Cord Blood-Derived Mesenchymal Stem Cells into Insulin-Producing Cells by PDX-1 mRNA Transfection. *Differentiation* **2014**, *87*, 200−208.

(19) Gautam, P.; Recino, A.; Foale, R. D.; Zhao, J.; Gan, S. U.; Wallberg, M.; Calne, R.; Lever, A. M. Promoter Optimisation of Lentiviral Vectors for Efficient Insulin Gene Expression in Canine Mesenchymal Stromal Cells: Potential Surrogate Beta Cells. *J. Gene. Med.* **2016**, *18*, 312−321.

(20) Kassem, D. H.; Kamal, M. M.; El-Kholy, E. L. G.; El-Mesallamy, H. O. Exendin-4 Enhances the Differentiation of Wharton's Jelly Mesenchymal Stem Cells into Insulin-Producing Cells through Activation of Various β-Cell Markers. *Stem Cell Res. Ther.* **2016**, *7*, 108.

(21) Lechner, A.; Yang, Y. G.; Blacken, R. A.; Wang, L.; Nolan, A. L.; Habener, J. F. No Evidence for Significant Transdifferentiation of Bone Marrow into Pancreatic β-cells. *Diabetes* **2004**, *53*, 616−623.

(22) Shree, N.; Bhonde, R. R. Conditioned Media from Adipose Tissue Derived Mesenchymal Stem Cells Reverse Insulin Resistance in Cellular Models. *J. Cell. Biochem.* **2017**, *118*, 2037−2043.

(23) Schorey, J. S.; Bhatnagar, S. Exosome Function: from Tumor Immunology to Pathogen Biology. *Traffic* **2008**, *9*, 871−881.

(24) Thomou, T.; Mori, M. A.; Dreyfuss, J. M.; Konishi, M.; Sakaguchi, M.; Wolfrum, C.; Rao, T. N.; Winnay, J. N.; Garcia-Martin, R.; Grinspoon, S. K.; Gorden, P.; Kahn, C. R. Adipose-Derived Circulating miRNAs Regulate Gene Expression in Other Tissues. *Nature* **2017**, *542*, 450−455.

(25) Garcia, N. A.; Moncayo-Arlandi, J.; Sepulveda, P.; Diez-Juan, A. Cardiomyocyte Exosomes Regulated Glycolytic Flux in Endothelium by Direct Transfer of GLUT Transporters and Glycolytic Enzymes. *Cardiovasc. Res.* **2016**, *109*, 397−408.

(26) Sun, W.; Hu, Q.; Ji, W.; Wright, G.; Gu, Z. Leveraging Physiology for Precision Drug Delivery. *Physiol. Rev.* **2017**, *97*, 189−225.

(27) Yameen, B.; Choi, W. I.; Vilos, C.; Swami, A.; Shi, J.; Farokhzad, O. C. Insight into Nanoparticle Cellular Uptake and Intracellular Targeting. *J. Controlled Release* **2014**, *190*, 485−499.

(28) Becker, A.; Thakur, B. K.; Weiss, J. M.; Kim, H. S.; Peinado, H.; Lyden, D. Extracellular Vesicles in Cancer: Cell-to-Cell Mediators of Metastasis. *Cancer Cell* **2016**, *30*, 836−848.

(29) Yan, Y.; Jiang, W.; Tan, Y.; Zou, S.; Zhang, H.; Mao, F.; Gong, A.; Qian, H.; Xu, W. HucMSC Exosome-Derived Gpx1 Is Required

DOI: 10.1021/acsnano.7b07643
ACS Nano 2018, 12, 7613−7628

for the Recovery of Hepatic Oxidant Injury. *Mol. Ther.* **2017**, *25*, 465−479.
(30) Li, T.; Yan, Y.; Wang, B.; Qian, H.; Zhang, X.; Shen, L.; Wang, M.; Zhou, Y.; Zhu, W.; Li, W.; Xu, W. Exosomes Derived from Human Umbilical Cord Mesenchymal Stem Cells Alleviate Liver Fibrosis. *Stem Cells Dev.* **2013**, *22*, 845−854.
(31) Zhou, Y.; Xu, H.; Xu, W.; Wang, B.; Wu, H.; Tao, Y.; Zhang, B.; Wang, M.; Mao, F.; Yan, Y.; Gao, S.; Gu, H.; Zhu, W.; Qian, H. Exosomes Released by Human Umbilical Cord Mesenchymal Stem Cells Protect Against Cisplatin-Induced Renal Oxidative Stress and Apoptosis *In Vivo* and *In Vitro*. *Stem Cell Res. Ther.* **2013**, *4*, 34.
(32) Zhang, B.; Shi, Y.; Gong, A.; Pan, Z.; Shi, H.; Yang, H.; Fu, H.; Yan, Y.; Zhang, X.; Wang, M.; Zhu, W.; Qian, H.; Xu, W. HucMSC Exosome-Delivered 14−3-3ζ Orchestrates Self-Control of the Wnt Response *via* Modulation of YAP During Cutaneous Regeneration. *Stem Cells* **2016**, *34*, 2485−2500.
(33) Reed, M. J.; Meszaros, K.; Entes, L. J.; Claypool, M. D.; Pinkett, J. G.; Gadbois, T. M.; Reaven, G. M. A New Rat Model of Type 2 Diabetes: the Fat-Fed, Streptozotocin-Treated Rat. *Metab., Clin. Exp.* **2000**, *49*, 1390−1394.
(34) Zhu, W.; Xu, W.; Jiang, R.; Qian, H.; Chen, M.; Hu, J.; Cao, W.; Han, C.; Chen, Y. Mesenchymal Stem Cells Derived from Bone Marrow Favor Tumor Cell Growth *In Vivo*. *Exp. Mol. Pathol.* **2006**, *80*, 267−274.
(35) Tatsumi, K.; Ohashi, K.; Matsubara, Y.; Kohori, A.; Ohno, T.; Kakidachi, H.; Horii, A.; Kanegae, K.; Utoh, R.; Iwata, T.; Okano, T. Tissue Factor Triggers Procoagulation in Transplanted Mesenchymal Stem Cells Leading to Thromboembolism. *Biochem. Biophys. Res. Commun.* **2013**, *431*, 203−209.
(36) Karussis, D.; Karageorgiou, C.; Vaknindembinsky, A.; Gowdakurkalli, B.; Gomori, J. M.; Kassis, M. I.; Bulte, J. W.; Petrou, P.; Ben-Hur, T.; Abramsky, O.; Slavin, S. Safety and Immunological Effects of Mesenchymal Stem Cell Transplantation in Patients with Multiple Sclerosis and Amyotrophic Lateral Sclerosis. *Arch. Neurol.* **2010**, *67*, 1187−1194.
(37) Mangi, A. A.; Noiseux, N.; Kong, D.; He, H.; Rezvani, M.; Ingwall, J. S.; Dzau, V. J. Mesenchymal Stem Cells Modified with Akt Prevent Remodeling and Restore Performance of Infarcted Hearts. *Nat. Med.* **2003**, *9*, 1195−1201.
(38) Liao, L.; Shi, B.; Chang, H.; Su, X.; Zhang, L.; Bi, C.; Shuai, Y.; Du, X.; Deng, Z.; Jin, Y. Heparin Improves BMSC Cell Therapy: Anticoagulant Treatment by Heparin Improves the Safety and Therapeutic Effect of Bone Marrow-Derived Mesenchymal Stem Cell Cytotherapy. *Theranostics* **2017**, *7*, 106−116.
(39) Camussi, G.; Deregibus, M. C.; Tetta, C. Paracrine/Endocrine Mechanism of Stem Cells on Kidney Repair: Role of Microvesicle Mediated Transfer of Genetic Information. *Curr. Opin. Nephrol. Hypertens.* **2010**, *19*, 7−12.
(40) Bang, C.; Thum, T. Exosomes: New Players in Cell-Cell Communication. *Int. J. Biochem. Cell Biol.* **2012**, *44*, 2060−2064.
(41) Simons, M.; Raposo, G. Exosomes Vesicular Carriers for Intercellular Communication. *Curr. Opin. Cell Biol.* **2009**, *21*, 575−581.
(42) Jiang, N.; Xiang, L.; He, L.; Yang, G.; Zheng, J.; Wang, C.; Zhang, Y.; Wang, S.; Zhou, Y.; Sheu, T.; Wu, J.; Chen, K.; Coelho, P. G.; Tovar, N. M.; Kim, S. H.; Chen, M.; Zhou, Y. H.; Mao, J. J. Exosomes Mediate Epithelium-Mesenchyme Crosstalk in Organ Development. *ACS Nano* **2017**, *11*, 7736−7746.
(43) Qiu, J.; Maekawa, K.; Kitamura, Y.; Miyata, Y.; Tanaka, K.; Tanaka, T.; Soga, M.; Tsuda, T.; Matsui, T. Stimulation of Glucose Uptake by Theasinensins through the AMP-Activated Protein Kinase Pathway in Rat Skeletal Muscle Cells. *Biochem. Pharmacol.* **2014**, *87*, 344−351.
(44) Sahin, K.; Onderci, M.; Tuzcu, M.; Ustundag, B.; Cikim, G.; Ozercan, I. H.; Sriramoju, V.; Juturu, V.; Komorowski, J. R. Effect of Chromium on Carbohydrate and Lipid Metabolism in a Rat Model of Type 2 Diabetes Mellitus: the Fat-Fed, streptozotocin-treated rat Streptozotocin-Treated Rat. *Metab., Clin. Exp.* **2007**, *56*, 1233−1240.
(45) Fraulob, J. C.; Ogg-Diamantino, R.; Fernandes-Santos, C.; Aguila, M. B.; Mandarim-de-Lacerda, C. A. A Mouse Model of Metabolic Syndrome: Insulin Resistance, Fatty Liver and Non-Alcoholic Fatty Pancreas Disease (NAFPD) in C57BL/6 Mice Fed a High Fat Diet. *J. Clin. Biochem. Nutr.* **2010**, *46*, 212−223.
(46) Zhu, Q.; Zhu, R.; Jin, J. Neutral Ceramidase-Enriched Exosomes Prevent Palmitic Acid-Induced Insulin Resistance in H4IIEC3 Hepatocytes. *FEBS Open Bio* **2016**, *6*, 1078−1084.
(47) Deng, Z.; Poliakov, A.; Hardy, R. W.; Clements, R.; Liu, C.; Liu, Y.; Wang, J.; Xiang, X.; Zhang, S.; Zhuang, X.; Shah, S. V.; Sun, D.; Michalek, S.; Grizzle, W. E.; Garvey, T.; Mobley, J.; Zhang, H. Adipose Tissue Exosome-Like Vesicles Mediate Activation of Macrophage-Induced Insulin Resistance. *Diabetes* **2009**, *58*, 2498−2505.
(48) Karlsson, H. K. R.; Zierath, J. R. Insulin Signaling and Glucose Transport in Insulin Resistant Human Skeletal Muscle. *Cell Biochem. Biophys.* **2007**, *48*, 103−113.
(49) Zhou, G.; Myers, R.; Li, Y.; Chen, Y.; Shen, X.; Fenyk-Melody, J.; Wu, M.; Ventre, J.; Doebber, T.; Fujii, N.; Musi, N.; Hirshman, M. F.; Goodyear, L. J.; Moller, E. E. Role of AMP-Activated Protein Kinase in Mechanism of Metformin Action. *J. Clin. Invest.* **2001**, *108*, 1167−1174.
(50) De Taeye, B. M.; Novitskaya, T.; McGuinness, O. P.; Gleaves, L.; Medda, M.; Covington, J. W.; Vaughan, D. E. Macrophage TNF-Alpha Contributes to Insulin Resistance and Hepatic Steatosis in Diet-Induced Obesity. *Am. J. Physiol. Endocrinol. Metab.* **2007**, *293*, E713−E725.
(51) Ying, W.; Riopel, M.; Bandyopadhyay, G.; Dong, Y.; Birmingham, A.; Seo, J. B.; Ofrecio, J. M.; Wollam, J.; Hernandez-Carretero, A.; Fu, W.; Li, P.; Olefsky, J. M. Adipose Tissue Macrophage-Derived Exosomal MiRNAs Can Modulate *In Vivo* and *In Vitro* Insulin Sensitivity. *Cell* **2017**, *171*, 372−384.
(52) Zisman, A.; Peroni, O. D.; Abel, E. D.; Michael, M. D.; Mauvaisjarvis, F.; Lowell, B. B.; Wojtaszewski, J. F.; Hirshman, M. F.; Virkamaki, A.; Goodyear, L. J.; Kahn, C. R.; Kahn, B. B. Targeted Disruption of the Glucose Transporter 4 Selectively in Muscle Causes Insulin Resistance and Glucose Intolerance. *Nat. Med.* **2000**, *6*, 924−928.
(53) Vendelbo, M. H.; Clasen, B. F.; Treebak, J. T.; Møller, L.; Krusenstjerna-Hafstrøm, T.; Madsen, M.; Nielsen, T. S.; Stødkilde-Jørgensen, H.; Pedersen, S. B.; Jørgensen, J. O.; Goodyear, L. J.; Wojtaszewski, J. F.; Møller, N.; Jessen, N. Insulin Resistance After a 72-h Fast Is Associated with Impaired AS160 Phosphorylation and Accumulation of Lipid and Glycogen in Human Skeletal Muscle. *Am. J. Physiol Endocrinol Metab.* **2012**, *302*, E190−E200.
(54) Leturque, A.; Brot-Laroche, E.; Le Gall, M. GLUT2Mutations, Translocation, and Receptor Function in Diet Sugar Managing. *Am. J. Physiol Endocrinol Metab.* **2009**, *296*, E985−E992.
(55) Tang, S.; Luo, F.; Feng, Y. M.; Wei, X.; Miao, H.; Lu, Y. B.; Tang, Y.; Ding, D. F.; Jin, J. F.; Zhu, Q. Neutral Ceramidase Secreted *via* Exosome Protects Against Palmitate-Induced Apoptosis in INS-1 Cells. *Exp. Clin. Endocrinol. Diabetes* **2017**, *125*, 130−135.
(56) Davidson, S. M.; Riquelme, J. A.; Takov, K.; Vicencio, J. M.; Boi-Doku, C.; Khoo, V.; Doreth, C.; Radenkovic, D.; Lavandero, S.; Yellon, D. M. Cardioprotection Mediated by Exosomes Is Impaired in the Setting of Type II Diabetes But Can Be Rescued by the Use of Non-Diabetic Exosomes *In Vitro*. *J. Cell. Mol. Med.* **2018**, *22*, 141−151.
(57) Jiang, Z. Z.; Liu, Y. M.; Niu, X.; Yin, J. Y.; Hu, B.; Guo, S. C.; Fan, Y.; Wang, Y.; Wang, N. S. Exosomes Secreted by Human Urine-Derived Stem Cells Could Prevent Kidney Complications from Type I Diabetes in Rats. *Stem Cell Res. Ther.* **2016**, *7*, 24.
(58) Xin, H.; Li, Y.; Liu, Z.; Wang, X.; Shang, X.; Cui, Y.; Zhang, Z. G.; Chopp, M. MiR-133b Promotes Neural Plasticity and Functional Recovery After Treatment of Stroke with Multipotent Mesenchymal StromalCells in Rats *via* Transfer of Exosome-Enriched Extracellular Particles. *Stem Cells* **2013**, *31*, 2737.
(59) Wen, D.; Peng, Y.; Liu, D.; Weizmann, Y.; Mahato, R. I. Mesenchymal Stem Cell and Derived Exosome as Small RNA Carrier

DOI: 10.1021/acsnano.7b07643
ACS Nano 2018, 12, 7613−7628

and Immunomodulator to Improve Islet Transplantation. *J. Controlled Release* **2016**, *238*, 166−175.
(60) Qiao, C.; Xu, W.; Zhu, W.; Hu, J.; Qian, H.; Yin, Q.; Xu, W. Human Mesenchymal Stem Cells Isolated from the Umbilical-Cord. *Cell. Biol. Int.* **2008**, *32*, 8−16.
(61) Van Deun, J.; Mestdagh, P.; Sormunen, R.; Cocquyt, V.; Vermaelen, K.; Vandesompele, J.; Bracke, M.; De Wever, O.; Hendrix, A. The Impact of Disparate Isolation Methods for Extracellular Vesicles on Downstream RNA Profiling. *J. Extracell. Vesicles* **2014**, *3*, 24858.
(62) Sun, L.; Xu, R.; Sun, X.; Duan, Y.; Han, Y.; Zhao, Y.; Qian, H.; Zhu, W.; Xu, W. Safety Evaluation of Exosomes Derived from Human Umbilical Cord Mesenchymal Stromal Cell. *Cytotherapy* **2016**, *18*, 413−422.
(63) Rachek, L. I.; Musiyenko, S. I.; Ledoux, S. P.; Wilson, G. L. Palmitate Induced Mitochondrial Deoxyribonucleic Acid Damage and Apoptosis in L6 Rat Skeletal Muscle Cells. *Endocrinology* **2007**, *148*, 293−299.
(64) Wiklander, O. P.; Nordin, J. Z.; O'Loughlin, A.; Gustafsson, Y.; Corso, G.; Mäger, I.; Vader, P.; Lee, Y.; Sork, H.; Seow, Y.; Heldring, N.; Alvarez-Erviti, L.; Smith, C. I.; Le Blanc, K.; Macchiarini, P.; Jungebluth, P.; Wood, M. J.; Andaloussi, S. E. Extracellular Vesicle *In Vivo* Biodistribution Is Determined by Cell Source, Route of Administration and Targeting. *J. Extracell. Vesicles* **2015**, *4*, 26316.

DOI: 10.1021/acsnano.7b07643
ACS Nano 2018, 12, 7613−7628